





ARTICLE

Prioritizing Watersheds for Intervention Design Using GIS and Remote Sensing

Endaweke Assegide^{1,2,3*} , Tena Alamirew^{1,3} , Claire L. Walsh⁴ , Gete Zeleke³ 

¹ Ethiopian Institute of Water Resource, Addis Ababa University, Addis Ababa P.O. Box 150461, Ethiopia

² School of Architecture and Engineering, Adama Science and Technology University, Adama P.O. Box 1888, Ethiopia

³ Water and Land Resource Center, Addis Ababa P.O. Box 3880, Ethiopia

⁴ School of Engineering, Newcastle University, Newcastle Upon Tyne NE1 7RU, UK

ABSTRACT

In many developing countries with poorly managed landscapes, soil erosion threatens the sustainability of water bodies. The main limitations of this study are the lack of daily sediment data, lithology, higher-resolution DEM data, and socioeconomic factors. Poor land use policy and resource management in the Upper Awash Sub-basin lead to soil erosion and sedimentation of hydrological infrastructure. Effective watershed prioritization requires integrating land use, hydrology, sediment load, and morphometric factors but often faces gaps, especially in the study area. This research aims to prioritise the Upper Awash Sub-Basin by its morphometric, land use and cover (LULC), and sediment yield characteristics. We used the integrated AHP-VIKOR multi-attribute decision-making method to prioritise watersheds, incorporating morphometry, LULC, and sediment load attributes in the simple matrix approach. The findings showed the following classes of erosion: exceedingly high (2722.14 km²), high (2524.46 km²), moderate (2205.48 km²), low (1611.43 km²), and extremely low (854.35 km²). Sub-watersheds WS6, WS8, WS10, WS13, and WS24 are the top priority for watershed management. The study ranked watersheds based on various attributes but encountered limitations such as the lack of daily sediment data, geological structure, and lithology. It can be concluded that this approach is very important to identify and categorize

*CORRESPONDING AUTHOR:

Endaweke Assegide, Ethiopian Institute of Water Resource, Addis Ababa University, Addis Ababa P.O. Box 150461, Ethiopia; School of Architecture and Engineering, Adama Science and Technology University, Adama P.O. Box 1888, Ethiopia; Water and Land Resource Center, Addis Ababa P.O. Box 3880, Ethiopia; Email: endawokassegid@yahoo.com

ARTICLE INFO

Received: 20 July 2024 | Revised: 13 August 2024 | Accepted: 19 September 2024 | Published Online: 25 November 2024

DOI: <https://doi.org/10.30564/jees.v7i1.6887>

CITATION

Assegide, E., Alamirew, T., Walsh, C.L., et al., 2024. Prioritizing Watersheds for Intervention Design Using GIS and Remote Sensing. Journal of Environmental & Earth Sciences. 7(1): 167–195. DOI: <https://doi.org/10.30564/jees.v7i1.6887>

COPYRIGHT

Copyright © 2024 by the author(s). Published by Bilingual Publishing Group. This is an open access article under the Creative Commons Attribution-NonCommercial 4.0 International (CC BY-NC 4.0) License (<https://creativecommons.org/licenses/by-nc/4.0/>).

hotspots of soil erosion sub-watersheds for planners and decision-makers for conserving water and soil and for different environmental management purposes.

Keywords: Morphometric Analysis; Soil Erosion; MCDM; VIKOR; AHP; SWAT

1. Introduction

Soil erosion and sediment-related challenges constitute a challenge for developing water resources and sustainable land management in many emerging nations^[1]. Problems with soil loss and sedimentation threaten the sustainability of land management and the development of water resources^[2]. Soil erosion is common in Ethiopia, and increased turbidity and sedimentation have an impact on some lakes^[3, 4]; soil erosion and sedimentation of hydrological infrastructure, especially artificial reservoirs used for power generation and water supply, are a result of the lack of a land use policy and poor resource management. In the Upper Awash Sub-basin, which has seen significant urbanization and deforestation, this is a common phenomenon^[5]. Because of the increasing amounts of silt deposition, lakes in the country's highland areas also confront issues with surface area, volume, and water level^[6]. Both the anticipated advantages of the dams and the significant costs incurred in their construction are lost as a result of reservoirs that were intended to deliver irrigation water and rapid sedimentation. On agricultural land, soil erosion affects water quality, ruins drainage systems, and reduces crop yield potential^[7]. Even though watershed degradation is believed to be the cause of the fast storage loss of Ethiopia's water-harvesting scheme and the loss of vital nutrients, few studies have been done to measure erosion rates and comprehend the dynamics of erosion-siltation processes at the catchment scale in terms of space^[8].

According to Hurni^[9], erosion in Ethiopia results in soil loss from cropland of $42 \text{ t ha}^{-1} \text{ y}^{-1}$. However, the complexity and unpredictability of the related land characteristics, for example, landscape, LULC, soils, and climate, affect the link between yearly sediment yield and drainage area^[8]. Furthermore, as population pressure rises quickly, deforestation, overgrazing, and intense subsistence farming may all play a significant role in soil erosion and degradation. Human activities in the environment as a whole, including modifications to methods of land use, can accelerate soil erosion^[11, 12]. This implies that if two catchments of comparable size have

distinct geomorphologies and climatic conditions, their sediment yield may vary. Depending on the local conditions and the geographical extent we are working with, the association between sediment yield and area may even alter between neighbouring places if the associated erosion processes and environmental variables are different^[8]. Both water erosion, higher temperatures (natural processes), urbanization, road construction, agriculture, industry, mining, and others (anthropogenic factors) have been identified as leading causes of soil erosion^[13, 14]. This indicates that before implementing practical connections discovered in other environmental conditions, it is necessary to evaluate the association between the catchment area and the measured area-specific sediment yield for local conditions^[15, 16]. The drainage pattern and runoff time necessary for a micro-watershed to focus at the outlet are controlled by the watershed's shape, which also influences the rate at which soil erosion and sediment generation occur^[17].

Because of soil erosion and sedimentation problems, the watersheds' ability to store water is reduced, dams and reservoirs are harmed, and surface waters are polluted^[18]. Consequently, sustaining and increasing resource production requires excellent planning and management of watersheds, especially making the best use of land in high-risk locations. The development, exploitation, and management of water and land resources are crucial for future generations' food security and population growth. It has previously been shown that this approach of all-encompassing watershed management heavily relies on watershed-based soil and water conservation techniques^[19]. SWC, if properly designed and carried out, has multiple positive effects on the environment and socio-economic system, in addition to lowering runoff and soil erosion, which is the main objective of tangible conservation measures^[20].

Ethiopia's highlands are some of Africa's most degraded regions^[21]. Ethiopia is experiencing alarming LULC changes, primarily driven by cultivation, leading to soil erosion and a decline in forests and grasslands^[22]. LULC in Ethiopia has changed significantly in the last 5 decades due to

the higher population growth rate and socioeconomic fluxes. The changes in population growth, overgrazing, and agricultural expansion in the highland areas have caused a drastic increase in the rate of LULC changes. LULC change causes significant impacts on water resources by causing alterations in the hydrological cycle^[21]. The LULC change detection study in the Upper Awash revealed declining trends in pasture, woodlands, and shrubland coverage, and a notable increase in cropland and urban areas, along with a higher conversion rate from shrubland to cropland. Urban area and farmland increased by 606.2% and 47.3%, respectively, between 1972 and 2014; in contrast, forests, pasture, shrubland, and water experienced declines of around 25%, 87%, and 29%, respectively. Many researchers have investigated the impact of LULC change on sediment yield dynamics in the Upper Awash. For example, according to Bihonegn^[21], streamflow, surface runoff, and sediment output increased by 4.55 %, 12.68 %, and 8.84 %, respectively due to the rapid change of LULC from 2000 to 2015.

The changing climate has the potential to exacerbate soil erosion^[11]. According to a study by Mitiku et al.^[23], the upper Awash Sub-basin's hydrological response to environmental and climate change has been impacted by increased annual and wet season river flows, with land use changes potentially leading to flooding. The results indicate that the annual and wet season monthly river flows increased by up to 77.5% and 100.5%, respectively, as a result of climate change. On the other hand, the change in land use affects river flow in a percentile increment or decrease of one.

Problems with soil erosion and water scarcity in the upper Awash Basin harm livelihoods and productivity. Even though some SWC interventions have been put into place in the region, it is unclear how beneficial these initiatives are and their impact is not extensively documented. Many smallholder farmers who depend on agriculture for their livelihoods live in this basin^[24].

Current land treatment procedures may not be feasible for large watersheds, making it difficult to manage the entire basin in a watershed management program^[25]. Since reducing the effects of natural disasters, management of all natural resources, including land and water, is essential to attaining sustainable development^[26]. Sub-watershed units are prioritised based on the degree of denudation caused by soil erosion and the criticality of drainage areas^[27]. Thus, the

integration of spatial analysis and satellite image approaches demonstrated a well-organized means that many researchers have successfully employed for studies on watershed management and development, along with the characterization and prioritization of watersheds^[28].

A watershed's prone areas can be identified and ranked in order of priority for mitigation measures using a variety of methodologies, including morphometric analysis, multi-criteria decision analysis, field surveys, and expert assessment^[29, 30]. Every approach has advantages and disadvantages. A field survey is a very precise method, but it has limitations since it takes a lot of expense and effort to collect the required data^[31]. Based on familiarity with and knowledge of the area, an expert view is an effective method for determining the locations affected by soil erosion. However, it's critical to remember that the quality of the output may suffer from insufficient data and competent specialists^[32]. A more straightforward and affordable approach is morphometric analysis, which results in reliable findings when consulted with experts^[29].

Rather than relying on watershed morphometry analysis, a more comprehensive approach that includes LULC and sediment load estimation is needed to characterize and prioritize sub-watersheds^[33]. Additionally, the prioritising approach permits the addition of LULC as a component to the morphometric parameters that may be introduced and that can have both direct and inverse impacts on the potential for erosion risk^[34, 35]. Ranking criteria may include morphometric variables, LULC, the average yearly soil loss, and other pertinent variables. To characterize and prioritize watersheds based on morphometric properties, LULC, and the degree of erosion or the load of sediment, remote sensing and GIS are essential^[36]. However, in this study, the absence of daily sediment data, lithology, and higher-resolution DEM data as well as socioeconomic factors like the construction of roads and buildings, and mining are the primary limitations of this work to be included as criteria.

An appropriate approach is required to integrate different parameters of multi-attribute for sub-watershed prioritization. The widely used multi-attribute decision-making (MADM) model, known as the Vise Kriterijumska Optimizacija Kompromisno Resenje (VIKOR), was first proposed by Opricovic^[37] and stressed the ranking and selection of numerous competing sets of criteria^[38]. Rather than deliv-

ering an ideal answer for a problem, the VIKOR technique finds a compromise solution for the conflicting attributes among numerous options^[37]. The VIKOR model is more accurate for prioritizing sub-watersheds, according to^[39, 40], due to this and the measure of “closeness to the ideal”, it was selected and implemented for this research work.

It is crucial to evaluate the amount of soil lost due to water erosion and its geographical distribution to successfully implement land and water conservation practices. In several regions of the world like the Pohru Watershed of the Jhelum Basin (Northwestern Himalayas)^[41], the Nagwan watershed, the Upper Damoder Valley Corporation (India)^[42], the Banha watershed (India)^[43], Ribb watershed (Ethiopia)^[44], and Finchaa Catchment (Ethiopia)^[45] SWAT has been used to analyze soil loss due to water erosion for watershed prioritizing purposes^[41]. The study also takes this research as a reference to implement the SWAT model.

The soil erosion in the upper catchments of the Awash River is one of the non-point pollution sources concerning agriculture. Water body and wetland pollution in the area are related to the erosion process. On crops, soil erosion lowers the yield potential, lowers the quality of the surface water, and damages the drainage network^[46]. Diffused pollutants and chemicals are also transported with soil particles, leading to increased sedimentation, eutrophication of the water, and tampering with fragile aquatic habitats^[7]. In addition to the previously noted issues, a watershed priority research project has never been done in the study area, even though there is a need for effective integration of land use, hydrology, sediment load, and morphometric factors. Therefore, to identify hotspots of soil erosion in watersheds and rank sub-watersheds according to their LULC, sediment yield, and morphometric characteristics of several drainage parameters for intervention design, the main objective of this research is to apply GIS and RS techniques in conjunction with multi-criteria decision-making (MCDM) like AHP-VIKOR and the SWAT model.

2. Study Area

One of Ethiopia's twelve major basins, the upper part of the Awash River Basin is the Upper Awash River Basin, which has an area of 9918.1 km². The upper Awash Sub-basin is situated between longitudes 37°57' E and 39°17'

E and latitudes 8°17' N and 9°18' N^[47]. The Omo Gibe and Rift Valley Lake Basins share the basin's western and southwest borders. The Abbay Basin is to the north and the Wabi Shebele Basin is to the southeast. The river begins in a location known as Elam near Ginchi town, south of Mount Warqe, at an elevation of 3000 meters above mean sea level (amsl). It then ascends to Koka Reservoir, located at an elevation of 1559.1 meters amsl. Its altitude variation range is between 1,591.1 to 3539.5 amsl. The Upper Awash River is a meandering river that flows for over 200 kilometers before entering Koka Reservoir (**Figure 1**)^[48]. Holeta, Alito, Teji, Gilo and Kelina, Kebena, Akaki, and Mojo are some of the river's principal tributaries. Upper Awash is home to significant agricultural farms, high vegetable production, and animal husbandry activities, primarily found in Addis Ababa, Adama, and Bishoftu^[7].

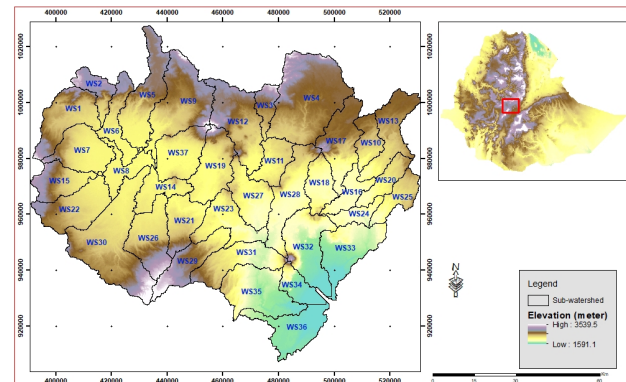


Figure 1. Study area, Upper Awash sub-basin.

This area is near the western escarpment of the major Ethiopian rift in the Ethiopian Highlands. This sub-basin is home to the significant Palaeolithic site Melka Kunture, which is well-known for its abundance of early hominid remains. The oldest documented use of obsidian, which comes from many outcrops surrounding the location, is at Melka Kunture. The area is characterized by its flat plateau terrain, with slopes primarily reaching 10°^[49]. The Awash River drains the research region to the east and southeast. The river flows into a canyon knick point (a waterfall) because of headward erosion occurring in the rift valley at a base level. Tectonic activity associated with rifting, including explosive volcanism, erosion, and sedimentation, was responsible for the creation of the terrain^[50]. Scarps that are visible display layers of ignimbrites and extensive lava flows. The area is characterized by a structural rift pattern, or graben and horst structure, which runs parallel to the semi-graben

fault system^[51]. The surrounding area of Melka Kunture has morphological evidence of the tectonic structure^[52].

The study area has a humid to sub-humid climate in the highlands and a semiarid environment in the lowlands, with an average annual temperature of 15–20 °C. The mean annual precipitation, strongly controlled by elevation, varies from 800 to 1400 mm. In Ethiopia, the primary wet season, Kiremt, typically occurs between June and September. It is followed by “Belg”, which occurs from March to May^[53].

3. Data and Method

3.1. Input Data

Different input data were used for this sub-watershed prioritization (Table 1). The strength of calibration is judged

relative to these benchmark values. Data on daily river flows were used to validate and calibrate the model^[47]. Sediment calibration and validation were conducted using monthly sediment data. It could be necessary to use different datasets to assess the SWAT model’s performance in different environmental scenarios^[54]. However, site-to-site variations may exist in the quantity of attributes and duration of observation needed for a suitable assessment of the driving processes of the watershed. There is a dearth of reliable, long-term data on the Ethiopian highlands. The full simulation period in this work is restricted to field observation data from 2002 to 2018 (validation) and 1979 to 2001 (calibration). To reduce the impact of non-equilibrium beginning circumstances, a five-year warm-up time was used for the split-sample calibration and validation^[55].

Table 1. Input data for the SWAT model and their sources.

Data	Resolution/Period	Source
Digital elevation model	30 meters	http://earthexplorer.usgs.gov/
Land cover	10-meters (2023)	https://earthexplorer.usgs.gov/ https://scihub.copernicus.eu/
Soil map	1:250000	Water and Land Resource Center
Climate	Rainfall, temperature wind speed, relative humidity, and solar radiation	National meteorological agency https://climatedataguide.ucar.edu/climate-data
Stream flow data	Observed daily	Ministry of Water and Energy
Sediment	Observed monthly	Ministry of Water and Energy

LULC is one of the features used for watershed prioritization. The major LULC is cropland followed by shrub land **Figure 2**.

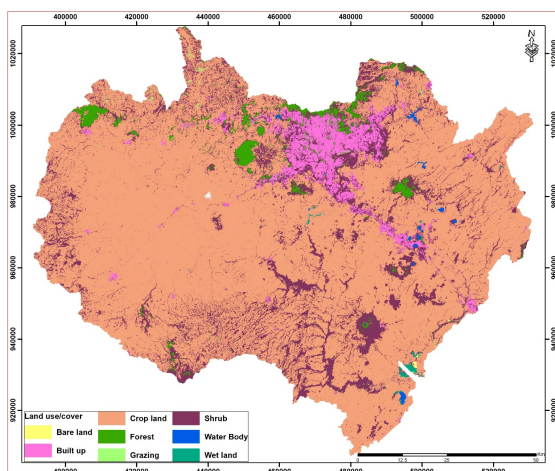


Figure 2. Map of land use and cover in the research area.

Different soil physicochemical and textural characteristics, such as bulk density, organic carbon content, hydraulic conductivity, and soil texture for various soil types’ layers, are needed for the SWAT hydrological model. This has been prepared and incorporated in the SWAT database for further analysis in the SWAT model. The dominant soil type in the study site is pellic vertisols (**Figure 3**).

3.2. Watershed Delineation and Morphometric Analysis

The sub-watershed ranking is the process of breaking down an entire watershed under investigation into smaller watershed units and assigning a score to each one based on priority for treatment^[56]. In ArcGIS software, the minimum area choice for sub-watersheds was set to 80 km² for watershed delineation. The Upper Awash sub-basin comprises 37 sub-

watersheds, from SW01 to SW37. The SW24 and SW04 sub-watersheds, which are the smallest and largest, respectively measure 98.35 and 681.71 km². The sub-watershed threshold area's average value is about 2.7% of the sub-basin total area. There is no detailed investigation and comparison done to set the threshold value of sub-watershed delineation in this research. The basis for choosing watershed delineation thresholds was based on other research works. Streamflow is not significantly affected by increasing the number of sub-watersheds. This is because the surface runoff is directly related to the CN, and CN is not markedly affected by the size of the sub-watersheds^[57]. Nevertheless, different study projects have varying threshold values for the size of the watershed area concerning soil erosion. Arabi et al.^[58] proposed an optimal watershed subdivision level for representation of the best management practices, corresponding to 2% of the total watershed areas and an average sub-watershed area of approximately 4%. Lin, Chen and Yao^[59] reported that the average sub-watershed area was approximately 1.6% of the entire watershed. For instance, the watershed area threshold proposed by Jha et al.^[57] indicates a range between 2% and 6% of the total drainage area, with a median value of 3%.

Three categories—linear, areal, and relief—generally comprise the morphometric characteristics. “Stream order,

number of streams, length, bifurcation ratio, drainage texture, relief ratio, drainage density, frequency, basin shape, form factor, circularity ratio, elongation ratio, and length of overland flow” are among the subcategories. Based on the stream hierarchy presented by Farhan et al.^[60] and Rahaman et al.^[61], the morphometric evaluation of drainage basins begins with the identification of stream order. The morphometric characterization of the designated sub-watersheds was computed using the method illustrated (Table 2).

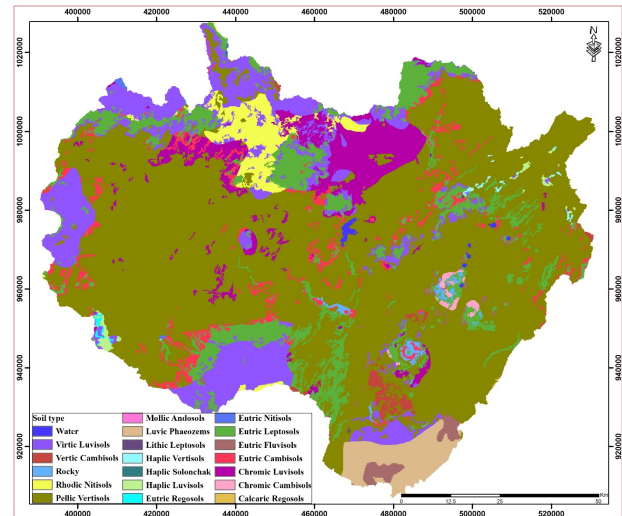


Figure 3. Soil type map of the study area.

Table 2. Algorithms used to calculate morphometric parameters and descriptions of parameters.

	Parameters	Algorithms/Definition	Source
Shape aspects	Watershed area (A)	Area within a watershed boundary (km ²)	[62]
	Perimeter (P)	The perimeter of the watershed (km)	[63]
	Basin length (L _b)	Length of the stream (km)	[63]
	Form factor (R _f)	$R_f = A/L_b$, where A = area of the basin (km ²) L_b^2 = square of the basin length	[63]
	Elongation ratio (R _e)	$R_e = 1.128 A L_b / P^2$, where, A = area of the basin (km ²) L _b = basin length	[64]
	Circularity ratio (R _c)	$R_c = 4 \times \pi \times A / P^2$ where, $\pi = 3.14$ A = area of the basin (km ²) P = perimeter (km)	[65]
Linear aspects	Mean stream length (L _{sm})	L_u / N_u (km) = L _{sm} , where L _{sm} is the mean stream length and L _u is the total length of each order's stream. N _u = total number of segments in the stream of order “u”	[64]
	Stream order (U)	Hierarchical rank	[66]
	Stream length ratio (R _L)	R _L is equal to L_u / L_{u-1} , and L_{u-1} is the whole stream length of its next lower-order	[63]
	Bifurcation ratio (R _b)	$R_b = N_u / N_{u+1}$, where N _{u+1} is the number of segments of the next higher order	[64]
	Mean bifurcation ratio (R _{bm})	R _{bm} is the average of all orders' bifurcation ratios.	[66]
	Drainage density (D _d)	D _d is the ratio of the total stream length of all orders (km) with the area of the watershed (km ²)	[63]
	Stream frequency (F _s)	F _s is the ratio of the total number of streams across all orders with the basin's area (km ²)	[67]
	Drainage texture (D _t)	D _t is the ratio of the total number of stream segments of order “u” with a perimeter of the watershed (km)	[68]

Table 2. Cont.

	Parameters	Algorithms/Definition	Source
Relief aspect	Relief ratio (Rr)	Rr is H/Lb , where, H is the total relief, Lb is the basin length	[69]
	Basin relief (Bh) or Total relief (H)	$Bh = h - h_1$, where, h = maximum height (m) h_1 = minimum height (m)	[64]
	Dissection index (Dis)	$Dis = Bh/Ra$, where, Ra = absolute relief Bh = basin relief	[70]
	Ruggedness number (Rn)	$Rn = Dd*(Bh/1000)$, where, Bh = basin relief, Dd = drainage density	[65]

3.3. LULC Analysis

LULC variations were mapped using the supervised classification method. Primarily, layer stacking and image subsetting using the study area boundary were made for Sentinel 2A image bands 10 m spatial resolution satellite imagery. Secondly, before the image classification, the LULC categories were decided from previous knowledge and field observation experiences as well as the visual inspection of the image. Then typical training areas for each LULC class were selected from homogeneous pixels of the satellite imagery. Finally, the maximum likelihood classification was implemented using the area of interest, and their areas were estimated. The 2023 LULC data was used as one factor to prioritize the sub-watersheds.

3.4. Sediment Load Analysis Using SWAT Model

The Soil and Water Assessment Tool (SWAT) is a continuous time, semi-distributed, basin-scale model developed for the USDA's Agricultural Research Service (ARS). The model was used to analyze the sediment load for sub-watershed priority^[71]; to evaluate and forecast the flow of water and sediment in large, ungauged basins; and the impacts of agricultural output on water, sediment, and agricultural chemical yields. It successfully enables the execution of long-term simulations^[72–74].

For conservation planning in a watershed, modeling and mapping of soil loss as well as risk assessment are crucial. The sub-watersheds are prioritized using how much soil loss occurs in each of their catchments. An empirical model called MUSLE is used to determine annual upland soil erosion^[75]. Five parameters are included in the MUSLE (Modified Universal Soil Loss Equation) that relate to rainfall, soil, landscape, LULC, and conservation efforts. SWAT integrates MUSLE with temporal elements of climate, base flow, and direct runoff to estimate sediment loading into

streams^[76].

MUSLE is a model that determines the maximum amount of sediment that can be routed in a reach based on peak channel velocity:

$$Sed_i = 11.8(Q_{surf} * q_{peak} * A_{hru})^{0.56} * K_{USLE} * C_{USLE} * P_{USLE} * LS_{USLE} * CFGR$$

The ArcGIS 5.1 extension, the graphical user interface for SWAT, and ArcSWAT version 10.21.10_5.24, released on August 19, 20, were used to develop the model setup. The stream definition was determined using the threshold area option, which specifies the minimum area of a sub-watershed, which was set at 8000 ha. In order to verify the comparability of observed and simulated data, one catchment outlet was manually inserted at this point in order to calibrate and validate flow and sediment data. Second, multiple HRUs were determined by applying a threshold of 20–10–20^[77] for the LULC, soil, and slope, as the most suitable standard to ascertain the quantity and kind of HRUs in every sub-watershed. HRU definition was based on the user-defined minimum percentage requirement determined by the user for each category. Thirdly, meteorological data was added to create data tables and an integrated database that was required for model setup and to mimic soil, weather, plant cover, management chores, and urban activities. Lastly, the start and end setup dates for the SWAT simulation technique from January 1979 to December 2019 were determined.

Sequential Uncertainty Fitting version 2 (SUFI-2), is an automated system that assesses the sensitivity and uncertainty analysis, parameterization, and calibration and validation of the hydrological parameters. The computational speed of this algorithm is very high. According to earlier tests, it performs better than the other algorithms in assessing uncertainty^[78, 79]. In this study, the SUFI-2 algorithm was utilized to assess the sensitivity of the model inputs^[78].

The P-factor in SUFI-2, which indicates the percentage of observations, runs from 0 to 100% in the calibration and validation, while the r-factor, which indicates the thickness

of the 95PPU, ranges from 0 to infinity^[79]. A simulation that exactly matches observed data has a p-factor of 1 and an r-factor of zero^[80], with a desirable r-factor value of less than 1^[79]. The strength of calibration is judged relative to these benchmark values. The model calibration and validation were conducted using daily river flow data^[47]. Monthly sediment data was utilized for calibration and validation purposes. Firstly, the hydrological component was calibrated and then the sediment component^[81].

3.5. (VIKOR) Method

The decision support system presented in this study employs the VIKOR technique, which tries to collect data on all information about several qualities and criteria^[82]. The VIKOR approach is applied as it makes it possible to choose extremely effective and efficient criteria when deciding how to proceed when there are multiple attributes and different criteria^[82, 83]. As the name indicates, the analytic hierarchy process (AHP) begins with the multi-attribute decision-making issue being broken down into a hierarchy mode. From there, weights can be found by mathematical calculations^[84]. Pair-wise comparisons are the basis of AHP, while Saaty^[85] provides its specifics.

Using the specified weights, VIKOR computes the compromise ranking list, compromise solution, and weight stability intervals for preference stability. When there are competing criteria, this strategy focuses on ranking and choosing from a group of choices. It presents the multi-criteria ranking index, which considers the relative importance of the distance to the ideal^[86, 87], and is determined by a specific metric for “closeness” to the “ideal” response^[37].

In the VIKOR approach, the steps below can be used to define options for rating^[38]:

1. Choosing the best decision among several options (Decision matrix):

$$D = \begin{bmatrix} a_{11} & a_{12} & a_{1n} \\ a_{21} & a_{22} & a_{2n} \\ \vdots & \vdots & \vdots \\ a_{m1} & a_{m2} & a_{mn} \end{bmatrix}$$

2. The linear approach to calculate the normalized decision matrix Equation (1):

$$n_{ij} = \frac{X_{ij}}{\sqrt{\sum_{i=1}^m x_{ij}^2}} \quad (1)$$

Where n_{ij} = the normalized matrix and ij = i th alternative in j th criteria.

3. Calculating the criteria's weight. The advantage of the VIKOR framework is that raw data can be used in addition to the elimination of the need for expert assessment for the evaluation of all criteria. The AHP approach was utilized in this study to determine the weight assigned to each criterion^[88].

The comparisons of two options pairwise using the given criterion can be used to create these weights. According to the specific criterion, the decision-maker evaluates the preference as weak, strong, very weak, or very strong^[89, 90]. As a result, it may be misleading to rank watersheds using a compound parameter. In this study, the weights of each morphometric parameter were determined using the AHP approach. AHP includes creating a matrix objectively and comparing each probable match. The elicitation of pairwise comparison judgments was the second step. Pairwise comparisons carried out at the fundamental scale shown in **Table 3** utilize the procedure outlined by Saaty^[91], which provides the scale to be applied in the assessments. The effectiveness of this scale has been attested by many users in numerous applications and theoretical comparisons with a vast array of other scales^[91]. Finally, ArcGIS was used to perform the spatial distribution of Erodibility prioritizing of sub-watersheds by the VIKOR technique using morphometric characteristics.

4. The procedure is multiplying each criterion's weight by the normalized matrix to get a weighted normalized matrix Equation (2).

$$V_{ij} = n_{ij} * w_j \quad (2)$$

5. Find the top (v_j^*) and the lowest (v_j^-) value: then $v_j^* = \max v_{ij}$ and $v_j^- = \min v_{ij}$. The top value (v_j^*) and the lowest value (v_j^-) are determined by picking the min and max values calculated by Equation (2) above. The best value (v_j^*) is the calculated max and the worst value (v_j^-) is the calculated min value.
6. Using Equations (3) and (4), respectively, to calculate the values of S_i (Utility Index) and R_i (Regret Index):

$$S_i = L_{1,i} = \sum_{j=1}^n W_j (v_j^* - v_{ij}) / (v_j^* - v_j^-) \quad (3)$$

$$R_i = L_{\infty,i} = \max \left[\sum_{j=1}^n W_j (v_j^* - v_{ij}) / (v_j^* - v_j^-) \right] \quad (4)$$

Where W_j is the weight of the criterion j .

7. Computing the values Q by Equation (5):

$$Q_i = V * \frac{(S_i - S^-)}{(S^* - S^-)} + (1 - V) * \frac{(R_i - R^-)}{(R^* - R^-)} \quad (5)$$

The strategy of maximum group utility, with v representing the strategy's maximum group utility and $(1 - v)$ representing individual regret, follows the majority rule when v exceeds 0.5. Within each sub-watershed, a high Q_i designates a higher priority and a lesser Q_i shows a less significant priority^[87].

The ranking index in VIKOR is determined using the opponent's least individual regret and maximum group utility^[40, 86]. In other words, the degree of similarity to the ideal choice may be compared to establish the compromise rating, provided that each alternative can be assessed using each criterion.

8. Prioritising the options included considering S , R , and Q values. Out of these three parameters, the optimal choice has the lowest value.

Table 3. The basic AHP rating used for pairwise comparison assessment.

Level of Significance	Meaning	Description
1	Equally significant	Each of the two activities contributes equally to the goal.
3	Moderately significant of one over another	One activity is moderately preferred over another by experience and judgment.
5	Strongly significant	Judgment and experience strongly preferred one activity over another.
7	Very strong significant	Activity is highly encouraged, and its superiority is shown practically.
9	Extreme significant	The strongest level of affirmation is seen in the data that supports a particular action over another.
2, 4, 6, 8	Values in the middle of the two adjacent judgments	While finding the middle ground is required.

Source: Saaty^[91].

3.6. Priority Index

Evaluating watersheds in order of importance or degradation involves analyzing each unique characteristic. Based on how susceptible they are to erosion watersheds were given priority in this study. Erosion risk assessment parameters are the morphometric variables Rb, Dd, Fs, Dt, Re, Cc, Bs, Rr, R, Rn, Rf, Lo, If, and SW^[19]. While form characteristics are inversely proportional to erodibility, linear morphometric parameters are directly proportional to it^[92]. The VIKOR approach was used to prioritize the weighted normalized decision matrix for morphometric parameters. The weighted normalized decision matrix for land use/cover was also taken into account using the VIKOR approach.

Sub-watersheds were ranked according to their morphometric parameters, taking into account their unique features. The VIKOR technique and a pairwise comparison matrix were used to rank the sub-watersheds in order of relevance or degradation. In this study, watersheds were prioritized based on their susceptibility to erosion^[34]. The susceptibility

was rated based on the condition indicator for morphometric, land use/cover, and sediment load parameter values for five priority index classifications as specified in **Table 4**.

The specifics of the complete procedure for ranking sub-watersheds along with morphometric factors were done while taking into account their unique properties. Based on how susceptible they are to erosion, watersheds were given a higher priority in this study^[34]. For example, watersheds with higher levels of several linear and relief morphometric criteria, including drainage density, stream frequency, overland flow length, basin relief, relief ratio, and roughness number, are particularly vulnerable to erosion due to high runoff and steeper slopes^[29].

To extrapolate a particular and related category LULC was further processed. For instance, all types of agricultural land were combined into a single attribute and given the name "cropland". The six LULCs that were taken into account throughout the ranking procedure were built-up, cultivated, forest, shrub, grass, and bare land. Wetlands and

water bodies were not taken into account in this work's rating process. The same process used to apply the morphometric parameters was used to apply the ranking technique for sub-watershed priority based on LULC. Additionally, as part of watershed prioritization, the sediment load from each watershed was taken into account. Prioritization of each sub-watershed was completed using priority index classification and quantitative data for each sub-watershed morphometric, LULC, and sediment load characteristics.

By taking two parameters at a time, the two-dimensional overlay matrices from the qualitative rating had been developed. First, morphometric data and land use/cover were analyzed as a matrix, and the results were divided into five classes that were then used for a second matrix analysis that included sediment load. Finally, they were divided into five qualitative categories once more. The group was chosen based on the risk assessment matrix in **Tables 4 and 5**, which

categorized all 37 sub-watersheds into five groups.

When employing a simple matrix method for prioritization, the morphometric, land use/cover, and sediment load variables were taken into consideration. The range of quantitative values for the qualitative value has been defined to set and create this matrix. The qualitative values of the morphometric, land use/cover, and sediment load parameter values are shown in **Table 6** as a condition indicator.

Five priority index classes^[95, 96] were established, with the sub-catchment with the lowest rating value indicating good environmental condition. In contrast, the sub-catchment having the best rating value in **Table 6** was provided with a very high priority designation and advised to undergo treatment immediately to control erosion.

The Q_i value indicates the Morphometric and Land use parameter values calculated using the VIKOR approach as condition indicators.

Table 4. Risk assessment matrix for identifying and determining priority aspects based on their ordinal values of arithmetic operation^[93].

*Ordinal		1	2	3	4	5
*Ordinal	Rating	VLP	LP	MP	HP	VHP
5	VLP	5	10	15	20	25
4	LP	4	8	12	16	20
3	MP	3	6	9	12	15
2	HP	2	4	6	8	10
1	VHP	1	2	3	4	5

Note: * Ordinal scale values refer to: 1—management not required in all cases; 2—management not required in most cases; 3—management required in some cases; 4—most cases require management attention; 5—requires immediate management attention. The numbers resulted from the product of ordinal values: 1–3 Very low (VLP); 4–6 Low (LP); 8–10 Medium (MP); 12–15 High (HP); >16 Very high (VHP). The ordinal scale values of the row and column are the same.

Table 5. Risk matrix with categories at the priority level determined by their qualitative value^[94].

Rating	VLP	LP	MP	HP	VHP
VHP	LP	MP	HP	VHP	VHP
HP	LP	MP	HP	VHP	VHP
MP	VLP	LP	MP	HP	HP
LP	VLP	LP	LP	MP	MP
VLP	VLP	VLP	VLP	LP	LP

Table 6. Condition indicator for morphometric, land use/cover, and sediment load parameter values.

Rank	Morphometric (Q_i)	Land Use (Q_i)	Sediment Yield ($t\ ha^{-1}\ year^{-1}$)
Very Low	>0.8	>0.9	0–5
Low	0.7–0.8	0.9–0.8	5–20
Medium	0.6–0.7	0.8–0.7	20–50
High	0.6–0.5	0.7–0.6	50–100
Very High	<0.5	<0.6	>100

4. Results

Priority analysis was carried out in this work using satellite imagery, DEM data, and the output of the SWAT model. Using various erosion hazard parameters, including morphometric parameters, LULC parameters, and sediment load, the multi-attribute decision-making (MADM) approach has been used in this investigation to identify priority sub-watersheds [26].

4.1. Sub-Watersheds Prioritization Using Morphometric Analysis

In the study location, dendritic and sub-dendritic drainage patterns were identified. The delimited layer area presented in **Table 7** and **Figure 1** was used to generate several fundamental parameters for the 37 watersheds. **Tables 8 and 9** shows the output of the morphometric analysis.

4.1.1. Fundamental Criteria

Area (A) is an area of a watershed as projected onto a horizontal plane. The area of the current study runs from 98.35 to 681.72 km², with SW04 having the least and SW24 having the greatest (**Table 7**).

The watershed perimeter (P) is the length of the defined watershed border. It also shows the extent of the catchment. The perimeter is between 241.55 and 78.09 km in length; the smallest length is SW30, while the longest one is SW34 (**Table 7**).

Watershed length (Lb) refers to the longest dimension of the basin in parallel with the principal discharge channel^[64]; it shows the primary waterway in the watershed, which transports the majority of the water. The longest sub-watershed in this regard is at SW03 (53.75 km), and the shortest is at SW24 (17.9 km) (**Table 7**).

Watershed relief (Bh) is the elevation between a catchment outlet and the highest point on its perimeter, and it varies from 1,591.11 to 3,538.6 m amsl.

Stream order (U) is a measure of a stream's position in the hierarchy of tributaries. The rivers are assigned an order using the Farhan approach^[60]. The sixth order is seen at SW23, SW31, SW34, and SW24. In the study area, SW08, SW14, SW16, SW21, SW23, SW24, SW27, and SW33 are of fifth order, whereas, SW23, SW31, SW35, and SW35 have sixth order. The entire upper Awash basin falls under

the sixth order (**Figure 4**).

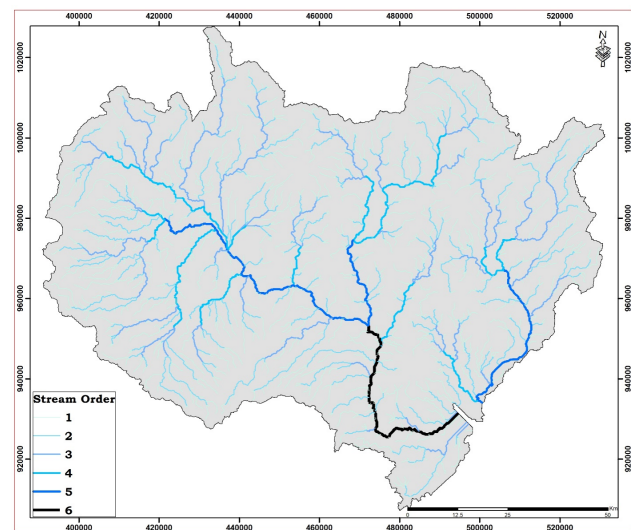


Figure 4. Stream order of Upper Awash basin.

Stream number (Nu) is used to describe how many stream segments are present in each sequence. With 71 first-order streams, WS04 was found to have the most, while WS03 had the fewest, with just 10 first-order streams (**Table 7**).

Stream length (Lu) is the mean distance of streams to each of the various orders. The stream lengths of all orders, both longest and shortest in the current research are SW30 (366.7 km) and SW24 (48.93 km), respectively (**Table 7**).

4.1.2. Linear Parameters

Bifurcation ratio (Rb) is a proportion of all rivers in an order (Nu) to all rivers in the next order (Nu + 1)^[64]. In the current study, SW31 (5.83) and SW24 (0.79) have the greatest and lowest Rb values, respectively. This suggests that SW24 and SW16 are comparatively sustainable sub-watersheds while SW31 and SW27 are relatively more disturbed than the others. Stream length ratio (Rl) is calculated by dividing the average river length of a given order (Lu) by the average river length of the subsequent lowermost order (Lu⁻¹) (Rl)^[63]. The relative rock formation permeability within a watershed and the historical evolution of stream segments are shown by the mean length of a stream's order remaining longer than that of the one below it. Two main principles govern how many streams and how long each stream order should be in a catchment area^[63].

Stream frequency (Fs), the ratio of the area of a watershed to all of its streams in all stream orders^[63]. Since they

Table 7. Computation of basic parameters for Upper Awash Basin (sub-watersheds).

WSID	Watershed Area (A) (km ²)	Watershed Perimeter (p) (km)	Stream Number (Nu)	Stream Length (Lu) Total	Basin Length (Lb)
WS1	320.15	132.41	67	161.1	34.99
WS2	130.73	96.78	29	58.4	21.04
WS3	101.52	83.88	19	49.8	18.22
WS4	681.72	177.29	141	342.4	53.75
WS5	366.14	187.91	85	190.5	37.76
WS6	185.06	151.91	31	94.4	25.63
WS7	275.09	120.84	55	170.5	32.10
WS8	153.32	160.79	27	89.0	23.03
WS9	472.60	204.29	97	235.9	43.65
WS10	137.05	90.18	25	67.2	21.61
WS11	167.42	104.40	37	83.9	24.21
WS12	395.84	163.91	87	206.1	39.47
WS13	284.69	164.33	53	134.7	32.73
WS14	156.70	121.56	32	72.0	23.32
WS15	203.10	111.24	47	127.8	27.02
WS16	130.66	111.06	29	63.6	21.03
WS17	308.41	152.99	69	150.7	34.26
WS18	166.62	91.98	40	89.5	24.15
WS19	301.11	135.05	67	154.8	33.79
WS20	136.44	94.74	27	73.1	21.55
WS21	218.69	110.22	36	110.0	28.18
WS22	316.64	133.43	55	194.8	34.77
WS23	252.38	158.15	50	122.6	30.57
WS24	98.35	94.08	23	48.9	17.90
WS25	151.23	96.12	31	83.2	22.85
WS26	309.31	131.75	65	180.6	34.31
WS27	245.15	123.60	55	113.9	30.07
WS28	338.04	175.43	72	188.2	36.09
WS29	241.22	136.73	42	116.8	29.79
WS30	656.66	241.55	131	366.7	52.62
WS31	284.76	135.23	48	161.0	32.74
WS32	350.96	145.37	67	193.4	36.86
WS33	328.11	144.77	68	198.1	35.48
WS34	130.16	78.90	18	83.7	20.99
WS35	377.57	165.89	73	193.6	38.43
WS36	271.38	161.63	46	132.2	31.85
WS37	273.08	106.74	62	185.4	31.97

often vary with drainage area size, the stream frequency values and drainage density for large and small drainage areas cannot be directly compared. However, drainage density and stream frequency are positively correlated, which suggests stream population and drainage density are increasing concurrently^[97, 98]. The watersheds' Fs values varied from 0.14 (SW18) to 0.24 (SW34), signifying substantial to moderate relief. It was discovered that in the watershed, Fs and Dd directly correlate.

Drainage density (Dd), the proportion of the total length of the current river to the area of the catchment^[63], is influenced by plant cover, permeability, and runoff potential. It represents the development of a watercourse and closeness

of proximity inside a sub-watershed^[99]. Among the 37 watersheds, WS37 had the highest drainage density (Dd = 0.68) and WS02 the lowest (Dd = 0.45). Extremely coarse drainage density in the studied area suggests that the watershed has poor hydrologic response and insufficient drainage. Gully erosion and flooding are major risks due to surface runoff is not being quickly removed from the watershed^[100].

Drainage Texture (Rt) indicates the comparative spacing of river channels. Mathematically, it is the total number of streams per perimeter of a watershed^[63, 68]. Rainfall, slope, subsurface permeability, vegetation, and climate all affect Rt. Based on the drainage texture, the sub-basin has been classified into four groups^[63]: coarse (Rt < 4), inter-

mediate ($R_t = 4-10$), fine ($R_t = 10-15$), and ultra-fine ($R_t > 15$).

Length of overland flow (L_o) is equal to the drainage density reciprocal divided by half. This quantity is essentially equivalent to the length of sheet flow and has a significant inverse connection with the mean channel slope. It describes how long water travels across the terrain before condensing into certain river channels. Greater surface runoff enters the stream when L_o is less. Even little rainfall is adequate to provide a large volume of surface runoff to stream discharge in terrain that is generally regular^[63, 101]. Infiltration number (I_f) is the product of stream frequency and drainage density. Greater infiltration numbers are correlated with higher surface runoff and low infiltration rates. The ratio of drainage density to stream frequency can be used to calculate the infiltration number^[102]. It and the infiltration rate have an inverse relationship. If values highlight areas of high relief and impermeable bedrock in the watershed and give information about infiltration characteristics^[102]. A low infiltration rate is indicated by a larger infiltration number, and vice versa.

4.1.3. Areal Parameters

Elongation Ratio (R_e), is the proportion of the watershed's greatest length to its circular diameter^[64]. It is used to evaluate a watershed's form. A lower value denotes a lengthy basin and a steep slope. It ranges from 0.4 to 1.0. Extremely low relief areas are characterized by R_e values near 1.0^[60]. R_e can be divided into four classes: circular (>0.9), oval (0.8–0.9), less elongated (0.7–0.8), and elongated (<0.7)^[100]. Typically, R_e has a value between 0 and 1, with 1 denoting a circular shape catchment and 0 denoting a severely elongated shape catchment. Among the 37 watersheds, WS24 ($R_e = 0.63$) had the greatest value, while WS04 and WS30 ($R_e = 0.55$) had the lowest. Circularity Ratio (R_c) is affected by the sub-watershed relief, slope, LULC, climatic change, stream length, stream frequency, and geological conditions. High R_c values indicate the catchment's stronger resemblance to a circular shape, which promotes consistent infiltration and a flow of excess water that lasts for a long time. Low R_c values indicate an extended watershed. Since a circular watershed will have the shortest concentration period, it is most

vulnerable to peak discharge. Lower, medium, and higher values of R_c represent the young, mature, and ancient phases of watershed development^[64, 103]. Form Factor (R_f) depicts the catchment shape and has an inverse relationship with erosion susceptibility^[67]. Lower R_f values imply stretched watersheds where water flows for extended periods with a flatter peak, while higher R_f values have high peak flows for shorter periods^[104].

Compactness Coefficient (C_c) represents the ratio of a watershed's perimeter to the circumference of a comparable circular area^[63]. The watershed's slope influences it, but not its extent. A lower C_c value denotes greater runoff and erodibility. In a circular basin, the drainage system will provide the least concentration time before the peak flow event becomes a greater risk^[92, 105].

4.1.4. Relief Parameters

The Relief Ratio (R_h) is basin relief (the variation in height between the highest and lowest) divided by the longest drainage distance of the catchment. It evaluates a watershed's overall steepness and measures the rate and severity of erosion on its slopes^[64]. Channel gradient and relief are directly correlated. R_h of the watershed is strongly associated with several hydrological features.

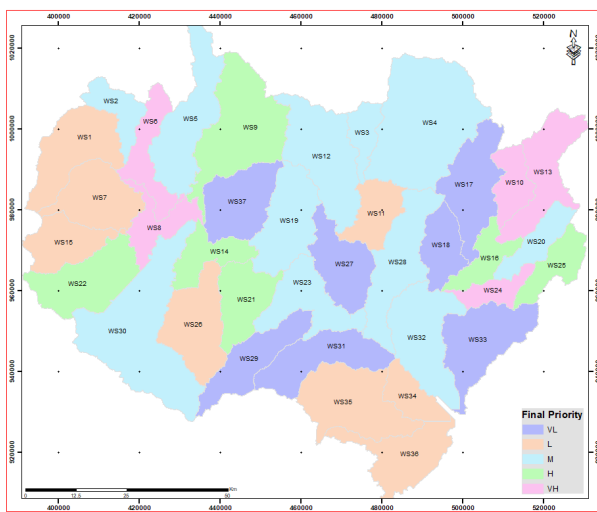
Ruggedness number (R_n) is drainage density multiplied by basin relief^[65]. R_n measures how uneven the catchment's surface is and illustrates the clear relationship between erosion and R_n . It combines the length and steepness of the slope. It establishes a relationship between the slope's length and steepness^[70, 106].

4.1.5. Pairwise Comparison Matrix Using AHP

Comparisons between pairs of options under the specified standard in **Table 8** make it possible to define the weights of the morphometric factors. The decision-maker judges each preference according to the criterion: very strong, strong, weak, or very weak. Apply inverses, that is, from 1/9 ("extremely not preferred") to 1 ("equally preferred"). **Table 8** shows that if we think one choice is less desirable than another on a criterion^[89, 90]. The elicitation of pairwise comparison judgments and scale was, as mentioned in Section 3.5 and **Table 3**.

Table 8. Calculated criterion weight values (using AHP) and pairwise comparison matrix for morphometric parameters.

	Rb	Fs	Dd	Dt	Rc	Re	Rf	Cc	Rr	R	Bs	SW	Rn	Lo	If
Rb	1	2	2	5	5	6	5	5	9	9	9	9	5	9	9
Fs	0.50	1	3	5	3	5	5	6	4	5	9	9	5	9	9
Dd	0.50	0.33	1	3	5	4	3	3	3	2	9	9	2	9	5
Dt	0.20	0.20	0.33	1	3	5	2	2	2	3	5	5	3	5	5
Rc	0.20	0.33	0.20	0.33	1	2	2	2	2	2	3	3	1	3	5
Re	0.17	0.20	0.25	0.20	0.50	1	2	2	2	2	3	3	2	3	9
Rf	0.20	0.20	0.33	0.50	0.50	0.50	1	2	2	2	5	5	2	5	4
Cc	0.20	0.17	0.33	0.50	0.50	0.50	0.50	1	2	2	3	3	2	3	3
Rr	0.11	0.25	0.33	0.50	0.50	0.50	0.50	0.50	1	2	3	3	2	3	2
R	0.11	0.20	0.50	0.33	0.50	0.50	0.50	0.50	0.50	1	3	3	2	3	2
Bs	0.11	0.11	0.11	0.20	0.33	0.33	0.20	0.33	0.33	0.33	1	2	1	2	2
SW	0.11	0.11	0.11	0.20	0.33	0.33	0.20	0.33	0.33	0.33	0.5	1	1	2	2
Rn	0.20	0.20	0.50	0.33	1.00	0.50	0.50	0.50	0.50	0.50	1	1	1	2	2
Lo	0.11	0.11	0.11	0.20	0.33	0.33	0.20	0.33	0.33	0.33	0.50	0.50	0.50	1	2
If	0.11	0.11	0.20	0.20	0.20	0.11	0.25	0.33	0.50	0.50	0.50	0.50	0.50	0.50	1
Weight	22.4	18.5	12.5	8.5	5.6	5.6	5.6	4.3	3.8	3.5	2	1.8	2.9	1.5	1.4

**Figure 5.** Priority map for sub-watersheds using morphometric parameters.

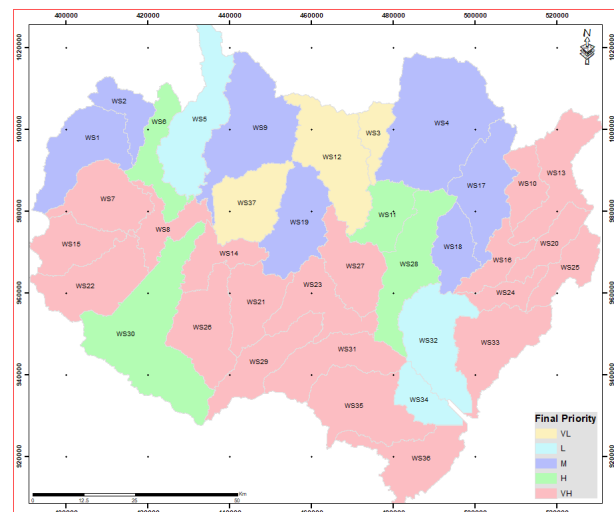
The bold font in **Table 9**, the column value derived according to the equation in **Table 1**, shows the sub-watersheds greater and lower values for every variable. Finally, ArcGIS is used to complete the spatial distribution of erodibility priority of each drainage area by the AHP-VIKOR technique using morphometric parameters.

4.2. Defining Sub-Watershed Priorities Using LULC Analysis

Eight main classifications comprise the LULC categories: bare ground, cropland, shrubland, water body, forest, built-up area, and grassland. A LULC classification accuracy assessment for the respective periods was made using local familiarity with the research area and Google Earth visuals. The overall accuracy of the classification was 91.2%. These are the classes that were taken into consideration for sub-watershed prioritization, except the water body and wetland

classifications.

Table 10 displays the ranking of thirty-seven sub-watersheds based on LULC using the AHP-VIKOR method. The watershed prioritization LULC parameter was based on the value range of the condition indicator in **Table 6**. Sub-catchments with high Qi values are most susceptible to soil loss (high priority), while those with low Qi values are least vulnerable (low priority). Finally, the spatial distribution of erodibility ranking of catchments by the AHP-VIKOR technique using LULC parameters was done using ArcGIS, as shown in **Figure 6**.

**Figure 6.** Priority map of sub-watersheds based on LULC parameter.

Pairwise Comparison Matrix Using AHP

The decision maker generates weights through pairwise comparisons of two alternatives, judging weak, strong, very weak, or very strong preferences under specific criteria^[89, 90], as discussed in Section 3.5, **Table 11**, and Section 4.1.5.

Table 9. Using morphometric parameters, the AHP-VIKOR technique prioritizes the erodibility of sub-watersheds at $v = 0.5$.

WSID	Rn	Rr	Rb	Dd	Fs	Bs	Dt	Rc	Re	Rf	Cc	R	Lo	If	S _i	R _i	Q _i
WS01	0.55	31.01	2.18	0.50	0.21	3.82	0.51	0.23	0.58	0.26	2.09	1085.1	0.99	0.42	0.56	0.16	0.54
WS02	0.43	46.29	1.63	0.45	0.22	3.39	0.30	0.18	0.61	0.30	2.39	973.9	1.12	0.50	0.56	0.19	0.66
WS03	0.52	58.14	1.83	0.49	0.19	3.27	0.23	0.18	0.62	0.31	2.35	1059.6	1.02	0.38	0.58	0.18	0.64
WS04	0.55	20.37	1.88	0.50	0.21	4.24	0.80	0.27	0.55	0.24	1.92	1094.9	1.00	0.41	0.56	0.18	0.61
WS05	0.45	22.76	1.54	0.52	0.23	3.89	0.45	0.13	0.57	0.26	2.77	859.4	0.96	0.45	0.58	0.19	0.69
WS06	0.41	31.55	1.61	0.51	0.17	3.55	0.20	0.10	0.60	0.28	3.15	808.7	0.98	0.33	0.69	0.19	0.84
WS07	0.68	34.36	2.02	0.62	0.20	3.75	0.46	0.24	0.58	0.27	2.06	1102.9	0.81	0.32	0.52	0.17	0.52
WS08	0.05	4.10	1.57	0.58	0.18	3.46	0.17	0.07	0.61	0.29	3.66	94.5	0.86	0.30	0.68	0.19	0.83
WS09	0.66	30.27	1.61	0.50	0.21	4.03	0.47	0.14	0.56	0.25	2.65	1321.5	1.00	0.41	0.61	0.19	0.72
WS10	0.31	29.17	1.58	0.49	0.18	3.41	0.28	0.21	0.61	0.29	2.17	630.3	1.02	0.37	0.66	0.19	0.80
WS11	0.19	15.78	2.09	0.50	0.22	3.50	0.35	0.19	0.60	0.29	2.28	382.0	1.00	0.44	0.58	0.17	0.59
WS12	0.70	33.87	1.67	0.52	0.22	3.94	0.53	0.19	0.57	0.25	2.32	1336.9	0.96	0.42	0.55	0.18	0.63
WS13	0.31	20.12	1.54	0.47	0.19	3.76	0.32	0.13	0.58	0.27	2.75	658.6	1.06	0.39	0.69	0.19	0.85
WS14	0.16	15.13	1.83	0.46	0.20	3.47	0.26	0.13	0.61	0.29	2.74	352.9	1.09	0.44	0.66	0.18	0.75
WS15	0.67	39.68	1.57	0.63	0.23	3.59	0.42	0.21	0.60	0.28	2.20	1072.0	0.79	0.37	0.47	0.19	0.53
WS16	0.27	26.32	1.29	0.49	0.22	3.39	0.26	0.13	0.61	0.30	2.74	553.5	1.03	0.46	0.61	0.20	0.78
WS17	0.59	35.13	2.36	0.49	0.22	3.80	0.45	0.17	0.58	0.26	2.46	1203.4	1.02	0.46	0.54	0.15	0.48
WS18	0.51	39.23	2.15	0.54	0.24	3.50	0.43	0.25	0.60	0.29	2.01	947.3	0.93	0.45	0.46	0.16	0.40
WS19	0.71	40.60	1.73	0.51	0.22	3.79	0.50	0.21	0.58	0.26	2.20	1372.1	0.97	0.43	0.54	0.18	0.60
WS20	0.36	31.08	1.68	0.54	0.20	3.41	0.29	0.19	0.61	0.29	2.29	670.0	0.93	0.37	0.60	0.18	0.69
WS21	0.46	32.61	1.94	0.50	0.16	3.63	0.33	0.23	0.59	0.28	2.10	919.0	0.99	0.33	0.68	0.17	0.75
WS22	0.49	22.79	1.78	0.62	0.17	3.82	0.41	0.22	0.58	0.26	2.12	792.6	0.81	0.28	0.63	0.18	0.72
WS23	0.40	26.70	1.97	0.49	0.20	3.70	0.32	0.13	0.59	0.27	2.81	816.3	1.03	0.41	0.63	0.17	0.67
WS24	0.29	32.49	0.79	0.50	0.23	3.26	0.24	0.14	0.63	0.31	2.68	581.5	1.01	0.47	0.58	0.22	0.84
WS25	0.39	31.43	1.57	0.55	0.20	3.45	0.32	0.21	0.61	0.29	2.21	718.2	0.91	0.37	0.59	0.19	0.70
WS26	0.62	31.16	1.95	0.58	0.21	3.81	0.49	0.22	0.58	0.26	2.11	1069.3	0.86	0.36	0.54	0.17	0.55
WS27	0.47	33.80	5.03	0.46	0.22	3.69	0.45	0.20	0.59	0.27	2.23	1016.4	1.08	0.48	0.43	0.12	0.17
WS28	0.72	35.59	1.67	0.56	0.21	3.85	0.41	0.14	0.57	0.26	2.69	1284.5	0.90	0.38	0.57	0.18	0.65
WS29	0.81	56.23	3.75	0.48	0.17	3.68	0.31	0.16	0.59	0.27	2.48	1675.3	1.03	0.36	0.55	0.13	0.39
WS30	0.83	28.27	1.69	0.56	0.20	4.22	0.54	0.14	0.55	0.24	2.66	1487.6	0.90	0.36	0.59	0.18	0.68
WS31	0.66	35.59	5.83	0.57	0.17	3.76	0.35	0.20	0.58	0.27	2.26	1165.2	0.88	0.30	0.45	0.13	0.25
WS32	0.77	38.12	1.82	0.55	0.19	3.87	0.46	0.21	0.57	0.26	2.19	1405.3	0.91	0.35	0.58	0.18	0.65
WS33	0.32	14.85	2.54	0.60	0.21	3.84	0.47	0.20	0.58	0.26	2.25	527.0	0.83	0.34	0.54	0.15	0.45
WS34	0.90	66.81	3.92	0.64	0.14	3.38	0.23	0.26	0.61	0.30	1.95	1402.0	0.78	0.22	0.49	0.19	0.55
WS35	0.39	19.72	2.41	0.51	0.19	3.91	0.44	0.17	0.57	0.26	2.41	757.9	0.97	0.38	0.63	0.15	0.59
WS36	0.18	11.58	2.86	0.49	0.17	3.74	0.28	0.13	0.58	0.27	2.77	369.0	1.03	0.35	0.69	0.13	0.59
WS37	0.90	41.38	3.34	0.68	0.23	3.74	0.58	0.30	0.58	0.27	1.82	1323.0	0.74	0.33	0.33	0.11	0.00

Table 10. Erodibility prioritization of sub-watershed by AHP-VIKOR method (at $v = 0.5$) using LULC.

WSID	Fst	Grl	Shl	Crl	Bar	Bup	Si	Ri	Qi
WS01	9.34	0.06	10.80	78.75	-	1.06	0.81	0.28	0.72
WS02	2.73	0.74	17.31	78.27	-	0.95	0.79	0.28	0.70
WS03	20.05	0.24	22.14	6.53	0.06	50.96	0.45	0.28	0.37
WS04	4.27	0.20	25.30	55.98	0.07	13.44	0.80	0.28	0.71
WS05	1.79	1.01	14.72	81.30	0.03	1.16	0.77	0.28	0.68
WS06	0.77	0.50	9.85	88.27	0.08	0.54	0.87	0.28	0.83
WS07	-	0.04	3.82	95.99	-	0.15	0.96	0.30	0.99
WS08	-	-	0.70	98.67	-	0.63	0.97	0.30	1.00
WS09	8.54	0.01	18.25	70.06	0.07	3.06	0.81	0.28	0.72
WS10	-	-	10.44	87.93	0.16	1.45	0.95	0.30	0.98
WS11	-	-	19.41	60.62	0.17	19.49	0.84	0.30	0.88
WS12	6.77	0.05	23.95	29.49	0.04	39.12	0.68	0.25	0.44
WS13	-	-	10.40	88.69	0.00	0.45	0.94	0.30	0.97
WS14	0.05	-	2.67	97.11	-	0.17	0.97	0.29	0.99
WS15	-	-	18.50	80.92	-	0.58	0.94	0.30	0.97
WS16	0.07	-	12.77	83.88	-	2.82	0.94	0.29	0.97
WS17	1.89	-	13.38	82.00	0.01	1.54	0.91	0.27	0.76
WS18	3.28	-	19.50	59.32	0.02	15.63	0.84	0.27	0.71
WS19	1.88	-	11.20	81.60	-	5.26	0.91	0.27	0.79
WS20	-	-	7.65	92.08	-	0.27	0.96	0.30	0.99

Table 10. Cont.

WSID	Fst	Grl	Shl	Crl	Bar	Bup	Si	Ri	Qi
WS21	-	-	7.14	92.63	-	0.21	0.96	0.30	0.99
WS22	0.00	-	8.66	90.68	-	0.65	0.96	0.30	0.99
WS23	-	-	19.01	80.46	0.01	0.45	0.94	0.30	0.97
WS24	0.06	-	8.92	89.82	0.11	1.09	0.95	0.29	0.98
WS25	0.67	-	8.48	90.14	0.03	0.67	0.95	0.29	0.91
WS26	0.09	-	9.94	89.51	0.00	0.43	0.95	0.29	0.97
WS27	0.16	-	12.59	86.59	-	0.14	0.91	0.29	0.93
WS28	2.34	-	12.69	82.14	-	2.82	0.91	0.28	0.81
WS29	0.39	0.05	28.52	70.23	0.03	0.79	0.91	0.29	0.91
WS30	1.05	0.02	12.00	86.34	-	0.59	0.93	0.28	0.87
WS31	0.09	0.02	23.68	75.76	0.10	0.29	0.93	0.29	0.95
WS32	0.99	-	18.93	77.36	0.57	0.44	0.73	0.28	0.67
WS33	0.00	-	13.58	81.98	1.09	2.92	0.87	0.29	0.91
WS34	0.16	-	20.17	77.09	0.01	0.03	0.66	0.29	0.69
WS35	0.02	-	29.73	69.62	0.45	0.07	0.92	0.29	0.95
WS36	-	-	6.60	91.05	0.00	0.34	0.90	0.30	0.94
WS37	5.33	-	5.99	86.93	-	0.92	0.79	0.22	0.33

Table 11. Pairwise comparison matrix and calculated criteria weight values (using AHP) for land use/cover parameters.

	Buy	Wel	Fst	Grl	Shl	Crl	Bar
Bup	1	1	2	2	7	9	9
Wel	1.00	1	2	2	7	9	9
Fst	0.50	0.50	1	1	5	9	9
Grl	0.50	0.50	1.00	1	5	9	9
Shl	0.14	0.14	0.20	0.20	1	2	2
Crl	0.11	0.11	0.11	0.11	0.50	1	1
Bar	0.11	0.11	0.11	0.11	0.50	1.00	1
Weight (%)	17.5	27.5	29.5	14.6	5.5	3.1	2.3

4.3. Sub-Watershed Priorities Using Sediment Load Analysis

This study used measured monthly suspended sediment and daily streamflow to validate and calibrate the model. The hydrological component was calibrated, followed by the sediment component^[81].

Once the performance of the SWAT hydrological model was deemed satisfactory, it was calibrated and used to evaluate the sediment yield modelling. The p-value indicates that 0.82 of the monthly sediment for the calibration period and 0.76 for the validation period. The calculated r-factors for the monthly sediment yield were 0.71 for the calibration and 0.63 for the validation periods **Table 12**.

Watershed ranking was done using the results of the model sediment load study. The watershed ranking sediment load parameter was according to the value range of the condition indicator **Table 13**. Finally, the spatial distribution of erodibility was determined using ArcGIS based on the sediment load parameter **Figure 7**.

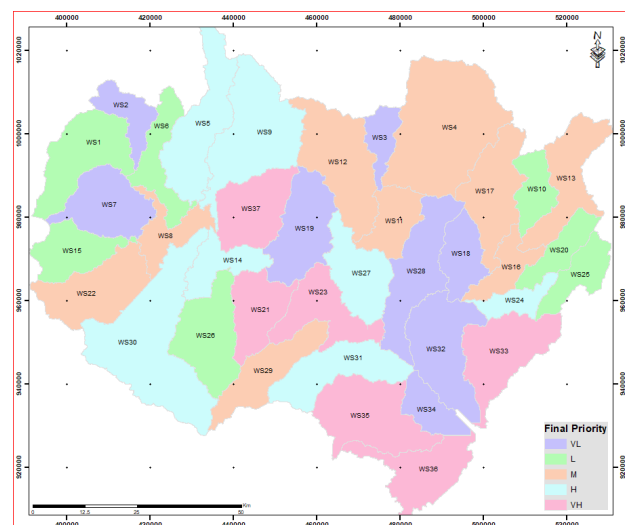


Figure 7. Priority map for sub-catchments based on the sediment load parameter.

4.4. Consistency Ratio (CR)

The consistency ratio is an index that shows the reliability of the decision-making. The concept of a consistency

Table 12. The performance of the SWAT model for streamflow and sediment during the calibration and validation phases.

Observatory		Period	P-Factor	R-Factor	PBIAS	RSR	R ²	NSE
Flow	Calibration	1979–2001	0.94	0.94	4.6	0.58	0.68	0.67
	Validation	2002–2018	0.92	0.8	5.4	0.57	0.68	0.67
Sediment	Calibration	1979–2001	0.82	0.71	−14.9	0.69	0.65	0.70
	Validation	2002–2018	0.76	0.63	20.8	0.55	0.63	−1.4

Table 13. Sub-watershed priority based on sediment load (t ha^{−1} year^{−1}).

WSID	Amount of Sediment (t y ^{−1})	WSID	Amount of Sediment (t y ^{−1})	WSID	Amount of Sediment (t y ^{−1})
WS01	1168.9	WS14	15125.5	WS26	2090.9
WS02	512.2	WS15	1884.6	WS27	11907.1
WS03	217.6	WS16	2547.4	WS28	835.5
WS04	3922.6	WS17	3751.5	WS29	2508.3
WS05	7157.9	WS18	348.9	WS30	7480.5
WS06	1478.7	WS19	717.8	WS31	12269.9
WS07	824.8	WS20	1273.1	WS32	979.3
WS08	3247.1	WS21	33031.9	WS33	13214.5
WS09	8308.2	WS22	3226.1	WS34	644.8
WS10	1601.7	WS23	40703.9	WS35	59823.9
WS11	3811.9	WS24	10816.5	WS36	47226.8
WS12	5617.9	WS25	1721.9	WS37	15475.5
WS13	3044.9				

metric is useless without the corresponding standards; according to Pant^[84], the limit is 0.10. To guarantee the judgments' credibility, the decision maker makes revisions to the decisions until a CR of less than 0.10^[91].

A pairwise comparison matrix was created by selecting fifteen morphometric factors directly or indirectly related to soil erosion and runoff for ranking sub-watersheds, as shown in **Table 8** for morphometric analysis and **Table 11** for LULC analysis, respectively. Next, to get the criterion weight values, all pairwise comparison matrix values were standardized for morphometric and LULC, respectively. For morphometric analysis and LULC analysis, the consistency ratio from the AHP analysis was determined to be 0.087 and 0.06, respectively. This indicates clearly that the criterion weight values are consistent and are less than 0.1.

4.5. Erodibility Prioritization

Setting priorities is a crucial component of any plan for managing watersheds to achieve beneficial outcomes and locating problem areas so that appropriate remedies using various soil and water conservation techniques can be found. Characterizing and prioritizing sub-watersheds requires a more comprehensive methodology that contemplates alter-

ations to the LULC and estimates of runoff and sediment production^[33]. In this research, based on the morphometric, LULC, and sediment load data, the combined AHP-VIKOR technique is used to prioritize the watersheds. The morphometric, LULC and sediment load values in **Table 7** were taken as a condition for prioritization using a simple matrix method. The integration process prepared a prioritized map by rescaling theme maps to five classes using the scores. Based on the range of condition indicator Qi value (VIKOR method), these micro-watersheds were classified as very high, high, medium, low, and very low.

Table 14 shows sub-watersheds with Qi values for morphometric and LULC parameters, respectively, ranging from 0.0 to 0.85 and 0.3 to 1.0. The final sub-watershed prioritized rank is shown in **Table 14**. The map in **Figure 8** shows the spatial distribution of the sub-catchments for land and water management work according to the grouped matrix evaluation of the morphometric, LULC, and sediment load parameters.

The results showed that 1611.43 km² (16.25%) in the category of extremely susceptible erosion, 2524.6 km² (25.45%) in the high susceptible class, 2722.14 km² (27.44%) in the moderate susceptible class, 854.35 km² (8.61%) in the class of low susceptible, and 2205.48 km²

(22.23%) in the class of very low susceptible. The percentage of sub-watersheds classified as low and very low priority for soil erosion is just 30% (12 sub-watersheds).

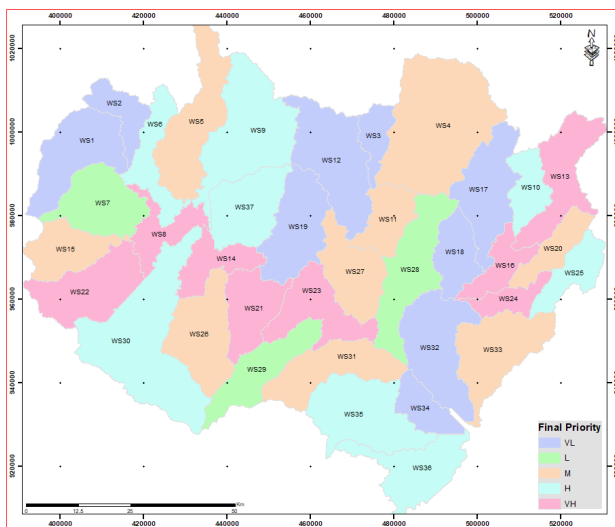


Figure 8. Erodibility prioritization of sub-watersheds.

5. Discussion

The Upper Awash Sub-basin is one of the most densely populated and urbanized parts of the country where the most populous cities such as Addis Ababa are located^[21]. If proper land use planning is not followed, the notable development in built-up regions and unplanned human settlements may increase the danger of environmental impairments^[107]. Higher urban sprawl is primarily brought about by the rapid rate of population growth, economic expansion, and accessibility to resources and essential infrastructure^[108]. Moreover, a high rate of soil erosion and a decline in the amount of arable land available are the results of a growing population^[22]. Soil erosion on agricultural land lowers crop yield potential, destroys drainage systems, and has an impact on water quality. The advantage of this research work is employing a comprehensive method for identifying and prioritizing sub-watersheds by incorporating morphometry, LULC, and sediment load, rather than relying solely on one watershed criteria analysis. Even though this study prioritized watersheds based on several attributes there were limitations like the lack of daily sediment data, geological structure, lithology, and socioeconomic issues such as road and building construction and mining.

Studies on sub-watershed prioritising in Ethiopia apply various techniques or methodologies. For example, Welde^[109], Dibaba, Demissie and Miegel^[45], Kefay, Abdisa

and Tumsa^[110] and Admas et al.^[44] prioritise Tekeze Dam watershed, Fincha catchment Blue Nile Basin, the middle Awata watershed in southern Ethiopia and Ribb watershed in Blue Nile Basin using SWAT, respectively; Jothimani, Lawrence and Dawi^[111] prioritized Megech River catchment, Blue Nile Basin, using morphometric analysis; Terefe et al.^[112] prioritized Ayu watershed, Abay basin, using the Revised Universal Soil Loss Equation (RUSLE) model and the Sub-Watershed Prioritization Tool (SWPT); Ketema and Dwarakish^[113] did prioritization in Tikur Wuha watershed based on soil loss rate; using the RUSLE model; Gashaw Tulu and Argaw^[114] and Abro^[115] defined priority to the Geleda watershed in the Blue Nile basin and the Gotu watershed in the Awash River basin, respectively; Godif and Manjunatha^[116] and Duressa et al.^[29] prioritized Geba river basin in Tigray and Dabus watershed in Blue Nile basin using morphometric parameters of the compound factor calculation approach, respectively; Gela^[117] prioritizes Gilgel Abay watershed, Blue Nile Basin using RUSLE model and morphometric parameters using compound factors approach.

While various Ethiopian watersheds have been prioritized using the aforementioned methodologies, the Upper Awash sub-basin, the research area, has not undergone any prioritizing efforts, furthermore, there is extremely little. Three distinct criteria—morphometric, LULC, and sediment load (as determined by the SWAT model)—are crucial in this case for watershed prioritizing using the AHP-VIKOR technique. GIS and RS approach alongside multi-attribute decision-making (MCDM) tools like AHP-VIKOR with a risk assessment matrix were used to prioritize the Upper Awash sub-basin, Ethiopia.

Prior research applying morphometric parameters for watershed prioritization led to the selection of each morphometric parameter employed in this study^[118]. Some of the fundamental criteria considered in the morphometric parameters are area, perimeter, watershed length, watershed relief, stream order, stream number, stream length, bifurcation ratio, stream length ratio, stream frequency, drainage density, drainage texture, length of overland flow, infiltration number, elongation ratio, circularity ratio, form factor, and compactness coefficient. As it accurately reveals the amount of water within a catchment, the area is an extremely important watershed property. Greater size intercepts more rainfall, more runoff, and higher peak discharge. Smaller sizes have

occasionally also seen the highest levels of flooding and sedimentation. Other watershed morphometric properties, such as stream networks, relief parameters, and shape and length are accountable.

Table 14. VIKOR index value and ranking method for prioritization of sub-watersheds at $v = 0.5$.

WSID	Morphometric				Land Use/Cover (LULC)				Sediment Load (SL)		Final Rank*
	S_i	R_i	Q_i	Rank	S_i	R_i	Q_i	Rank	SL ($t\ y^{-1}$)	Rank	
WS01	0.56	0.16	0.54	L	0.81	0.28	0.72	M	1169.0	L	VL
WS02	0.56	0.19	0.66	M	0.79	0.28	0.70	M	512.2	VL	VL
WS03	0.58	0.18	0.64	M	0.45	0.28	0.37	VL	217.6	VL	VL
WS04	0.56	0.18	0.61	M	0.80	0.28	0.71	M	3922.6	M	M
WS05	0.58	0.19	0.69	M	0.77	0.28	0.68	L	7157.9	H	M
WS06	0.69	0.19	0.84	VH	0.87	0.28	0.83	H	1478.7	L	H
WS07	0.52	0.17	0.52	L	0.96	0.30	0.99	VH	824.8	VL	L
WS08	0.68	0.19	0.83	VH	0.97	0.30	1.00	VH	3247.1	M	VH
WS09	0.61	0.19	0.72	H	0.81	0.28	0.72	M	8308.2	H	H
WS10	0.66	0.19	0.80	VH	0.95	0.30	0.98	VH	1601.7	L	H
WS11	0.58	0.17	0.59	L	0.84	0.30	0.88	H	3812.0	M	M
WS12	0.55	0.18	0.63	M	0.68	0.25	0.44	VL	5617.9	M	VL
WS13	0.69	0.19	0.85	VH	0.94	0.30	0.97	VH	3045.0	M	VH
WS14	0.66	0.18	0.75	H	0.97	0.29	0.99	VH	15125.5	VH	VH
WS15	0.47	0.19	0.53	L	0.94	0.30	0.97	VH	1884.6	L	M
WS16	0.61	0.20	0.78	H	0.94	0.29	0.97	VH	2547.4	M	VH
WS17	0.54	0.15	0.48	VL	0.91	0.27	0.76	M	3751.5	M	VL
WS18	0.46	0.16	0.40	VL	0.84	0.27	0.71	M	349.0	VL	VL
WS19	0.54	0.18	0.60	M	0.91	0.27	0.79	M	717.8	VL	VL
WS20	0.60	0.18	0.69	M	0.96	0.30	0.99	VH	1273.1	L	M
WS21	0.68	0.17	0.75	H	0.96	0.30	0.99	VH	33031.9	VH	VH
WS22	0.63	0.18	0.72	H	0.96	0.30	0.99	VH	3226.1	M	VH
WS23	0.63	0.17	0.67	M	0.94	0.30	0.97	VH	40703.9	VH	VH
WS24	0.58	0.22	0.84	VH	0.95	0.29	0.98	VH	10816.5	H	VH
WS25	0.59	0.19	0.70	H	0.95	0.29	0.91	VH	1721.8	L	H
WS26	0.54	0.17	0.55	L	0.95	0.29	0.97	VH	2090.9	L	M
WS27	0.43	0.12	0.17	VL	0.91	0.29	0.93	VH	11907.1	H	M
WS28	0.57	0.18	0.65	M	0.91	0.28	0.81	H	835.5	VL	L
WS29	0.55	0.13	0.39	VL	0.91	0.29	0.91	VH	2508.4	M	L
WS30	0.59	0.18	0.68	M	0.93	0.28	0.87	H	7480.5	H	H
WS31	0.45	0.13	0.25	VL	0.93	0.29	0.95	VH	12269.9	H	M
WS32	0.58	0.18	0.65	M	0.73	0.28	0.67	L	979.3	VL	VL
WS33	0.54	0.15	0.45	VL	0.87	0.29	0.91	VH	13214.5	VH	M
WS34	0.49	0.19	0.55	L	0.66	0.29	0.69	L	644.8	VL	VL
WS35	0.63	0.15	0.59	L	0.92	0.29	0.95	VH	59823.9	VH	H
WS36	0.69	0.13	0.59	L	0.90	0.30	0.94	VH	47226.8	VH	H
WS37	0.33	0.11	0.00	VL	0.79	0.22	0.33	VL	15475.5	VH	L

Note: * The value provided in **Tables 4** and **5** determines the final rank.

The first stage in morphometric analysis is to organize or categorize streams based on the quantity and kind of tributary connections. Since six is the highest stream order found in the sub-basin, the Upper Awash Basin belongs to the six-order type. An inverse geometric series is formed as a link between the stream order and the number of streams of a particular order^[63]. For instance, a watershed with a higher proportion of uppermost channels often has a topography that is highly permeable to infiltration. Soft shale and slate rocks are typical of a watershed where the quantity and arrangement of streams are increased^[119].

The uppermost channels have the largest lengths, and stream orders go up from there^[63]. Stream length varies

with the topography; longer streams are found in places with coarser textures and lower slopes, while shorter streams are found in areas with finer textures and steeper slopes^[60]. Additionally, it evaluates the hydrologic features and rock formation of the area. A lesser number of streams with longer lengths are formed relative to the porous rock layer and well-drained catchment, and vice versa^[120]. The study measures a total stream length of 366.7 km, 342 km, 235 km, and 206 km, corresponding to SW30, SW04, SW2, and SW12, in that order. These watersheds are the uppermost channels and it is considered that sediment can be carried out downstream. Because water flows more slowly in longer streams, sediment can settle out of the water column and be transferred

downstream over longer distances^[29].

Horton^[69] asserts that the bifurcation ratio (Rb) is connected to the drainage system's branching pattern, indicating the level of integration between streams of various orders. In basins without any structural influence and nearly level terrain, the Rb value is less than 3. When the Rb number falls between three and five, it indicates that the rock structure of the basin has less impact on the drainage network^[121]. Less structurally disrupted watersheds without any deformation in the river network are indicated by lesser Rb^[97, 122]. This implies that, in the study area, structural disruptions have not impacted the drainage network in nearly every catchment. SW16 is nearly flat and less structurally disturbed compared to SW31 which is highly dissected and structurally disturbed resulting in extensive erosion and sediment transportation.

High values of stream frequency (Fs) are used to represent steep surfaces with more surface runoff. A high Fs value indicates an impermeable underlying material, high relief conditions, and low infiltration capacity. That is to say, the larger value of Fs shows greater soil erosion (increased runoff)^[67].

Drainage texture varied from 0.8 to 0.17 in the current study, and all watersheds were categorized as coarse. Low infiltration capacity, an impermeable soil layer, and excessive runoff in the basins are indicated by the coarse drainage texture (Rt) values. The more stream segments in a basin, the more impermeable the surface is^[123].

The fact that the SW02 sub-catchment overland flow distance is lower than that of the other sub-watersheds suggests that the water travels through the land surface over a shorter distance. In contrast, the sub-catchment SW37 takes the highest value, suggesting that before being concentrated in stream channels, the water in SW37 tends to go farther across the land surface.

The highest infiltration number is found in SW02; this is associated with increased drainage density and overall stream frequency. This indicates that SW02 may have more opportunity for overland flow and a much lower rate of infiltration compared to the other sub-watersheds. The lowest infiltration value, on the other hand, is found in SW34, which denotes a lower total stream frequency and drainage density. This implies that SW34 may have a significantly greater penetration rate and a lower danger of overland flow than the sub-watershed. The study area is grouped as a low value

of Re (elongated watershed) and has high relief and a steep slope. The area can be characterized by a poor rate of infiltration with high runoff.

In the research area, SW37 has greater circulatory ratio values (0.30). The Rc value for Watershed WS8 was 0.07, which was the lowest. The sub-basin exhibits a range of Rc values from 0.07 to 0.3, which suggests that the geologic materials are homogeneous, highly permeable, and free of structural disturbances.

The Watershed form factor ranged from 0.31 (WS24 and WS03) to 0.24 (WS04 and WS30) in the research sub-basin. Sub-watersheds with low form factors have high peak flows over shorter periods, which increases their vulnerability to water-induced mechanical erosion. Watershed form factor values <0.78 are elongated whereas >0.78 are circular^[100]. Higher Rf values indicate higher peak flows over shorter periods, while lower Rf values indicate lower peak flows over longer periods^[63, 124].

In the current investigation, SW37 (1.82) has a lower compactness coefficient value than SW08 (3.66) but a higher compactness coefficient overall. The sub-watershed area and shape of SW04 and SW34 have lower values, while SW05, SW13, and SW23 take substantially greater values. The lower value of Cc indicates that WS37, WS04, and SW34 are most susceptible to erosion.

Relief Ratio (Rh) increases when drainage/stream area and watershed size decrease. It ties the overall slope of the drainage area to the steepness and soil erosion in the basin. Numerous studies have found a strong relationship between Rh and loss of sediment^[64, 123, 125]. The steepness (high slope)^[126] and elevated relief within the watershed are shown by the higher values of Rh. The runoff increases the likelihood of erosion in the basins with steeper slopes. The lower Rh value, on the other hand, denotes a low slope (steepness) and low relief. Rh values that are higher indicate severe slopes and higher relief. Rh = 66.81 was discovered to be the highest value that corresponds to WS34.

An extraordinarily high value of Rn arises under steep slopes^[102] and high Dd values when both factors are large. These basins have been assessed to be at risk of flooding. Rn's value ranged from 0.05 (for WS08) to 0.9 (for WS34 and WS37). Slopes have higher values when they are steep and longer. The study area has high values at SW29, SW30, SW34, and SW37, and lower values at SW08, SW14, and

SW36.

The higher VIKOR index (Q_i) value (**Table 9**) for morphometric parameters indicates the highest priority and the most vulnerable sub-watershed to soil loss, however the lowest Q_i value indicates the lowest priority and the least susceptible sub-watershed to soil erosion. The study area drainage has not been impacted by structural disturbances, as seen by low bifurcation ratio values and very low drainage densities for nearly all of its sub-watersheds. Additionally, the area is primarily covered by permeable and resistant formations^[127]. The loss of soil is influenced by morphometric factors such as form factor, elongation ratio, circularity ratio, and compactness coefficient in an inverse manner, and directly by bifurcation ratio, overland flow length, drainage density, texture, and stream frequency. This might be taken to suggest that for morphometric factors that have a direct correlation with soil erosion, larger values should be allocated a greater rank (lower values). The ruggedness number and relief ratio measures are directly correlated with soil degradation^[128]. As previously stated, sub-watersheds with higher soil erodibility are assigned higher priorities and the other way around.

In the VIKOR approach to determine the best and worst values of the morphometric parameters, to determine Q_i values, utility and regret metrics were computed. The result revealed that SW17, SW18, SW27, SW29, SW31, SW33, and SW37 are the most vulnerable watersheds to soil loss and other erosive factors, as shown in **Table 9** and **Figure 5**. Similarly, the Q_i ranges from 0.37 in WS03 to 1.0 in WS08 for the LULC parameter at $v = 0.5$. The result showed that SW03, WS12, and WS37 are the most vulnerable watersheds to soil loss and other erosive factors, as revealed in **Table 10** and **Figure 6**.

According to Abbaspour et al.^[129], the result indicates that the SWAT model accurately simulates streamflow. In line with the evaluation standards suggested by Moriasi et al.^[130], for the calibration and validation period, the PBIAS was very good, NSE was good and RSR was good, (**Table 12**). WS18 had the lowest sediment load ($2.09 \text{ t ha}^{-1} \text{ yr}^{-1}$) and an area of 166.62 km^2 , while WS35 had the highest sediment load ($174.02 \text{ t ha}^{-1} \text{ yr}^{-1}$) and an area of 271.38 km^2 .

Soil erosion is a complex process influenced by various factors including land use, climate, geology, and

management techniques. Prioritising using sediment load, LULC, and morphometric analysis showed that SW08, SW13, SW14, SW16, SW21, SW22, SW23, and SW24 sub-watersheds fall under very high priority, suggesting that the most susceptible watersheds are more vulnerable to soil erosion and other erosive agents; WS06, WS09, WS10, WS25, WS30, WS35, WS36, and WS37 are under high priority; WS04, WS05, WS11, WS15, WS20, WS26, WS27, WS31, and WS06, WS09, WS10, WS25, WS30, WS35, WS36, and WS37 medium priority; WS07, WS28 and WS29 low priority and WS01, WS02, WS03, WS12, WS17, WS18, WS19, WS32, WS34, and WS35 fall under very low priority concerning soil erosion, signifying that the low-priority sub-watersheds natural resources are less vulnerable to the damaging impacts of precipitation and other erosive agents as illustrated in **Table 14** and **Figure 8**.

The major reason behind this research is to identify and categorize hotspots of soil erosion within sub-watersheds. The finding has the added advantage of assisting planners and decision-makers in developing corrective actions for various environmental problems, such as managing floods, preventing soil erosion, enhancing water quality, managing natural resources, and implementing various conservation techniques. Furthermore, this research has advantages for large-scale projects, enabling planners and experts to choose strategies according to the size of the catchment area, the severity of the issue, available funds, and the needs of the local and governmental systems.

When implementing conservation techniques for soil and water, extra attention needs to be given to the high-priority sub-catchments. To prevent soil loss, rapid soil and water conservation techniques such as contour binding, bench terracing, gully control structures, and grass waterways are needed in sub-watersheds with high and very high erosion susceptibility. By slowing down runoff, preventing gully erosion, and holding onto sediment, these actions effectively control and stop water runoff and soil erosion^[122, 131].

The morphometric parameters' accuracy and specificity may have been limited by low-resolution DEM (30 meters), which might have led to an underestimation or incorrect description of erosion-prone locations. In addition to this, daily sediment data, lithology and socioeconomic factors may have similar contributions. As a result, future research direction is advised to incorporate sediment data, geological structure

or lithology, higher resolution DEM data than 30 meters and to improve accuracy for conservation efforts, acquire more accurate physical data for sediment yield simulations that are more trustworthy, and capture more details that can offer a more realistic representation of fine-scale features like small gullies, ridges, and ephemeral streams, which are essential for comprehending erosion patterns.

6. Conclusions

This research focuses on prioritizing sub-watersheds for intervention design using GIS and remote sensing techniques and the AHP-VIKOR Method. Land managers may develop specific measures that reduce soil erosion and safeguard water resources after determining each sub-watershed's susceptibility to soil erosion.

Natural and human-caused degradation in a drainage area can affect water resource initiatives and a nation's economy by lowering crop yield. As a result, a more comprehensive indicator of erosion risk in a watershed is the multiple values of morphometric parameters, LULC, and sediment load. For planners and decision-makers to comprehend the morphological, LULC, and sediment load characteristics of any particular sub-watershed for planning at the sub-catchment level, GIS and remote sensing approaches are more effective. The linear, areal, and relief features illustrate the watershed's hydrological characteristics, and their features are very helpful in demonstrating how each sub-watershed should be prioritized.

Multi-criteria decision-making (MCDM) techniques such as the analytical hierarchy process, weights of evidence, analytical network process, and evidential belief function may be used. However, these techniques are biased, lengthy, and have time-consuming computational procedures. To overcome these issues, fuzzy logic-based machine learning algorithms may be coupled with MCDM techniques. Thus, fuzzy logic and AHP-based land and water conservation (SWPC) models should be developed in the future.

High and extremely high-priority areas require the implementation of immediate management solutions, covering about 42% (16 sub-watersheds) of the sub-watersheds to decrease the potential for degradation. It is recommended that the required conservation action be taken to lower soil erosion and sediment yield in the sub-watersheds and reduce

sedimentation in the Koka reservoir, which is the study area's final outlet. This is due to the very high susceptibility of the Upper Awash Basin to soil erosion.

Author Contributions

E.A. was the primary investigator and lead author; he designed the method, developed the conceptual framework, wrote the first draft, and edited and reviewed subsequent drafts of the manuscript. The supervision and funds acquisition were aided by G.Z. and T.A.. Multiple early drafts of the paper were revised and reviewed by T.A. and C.L.W.

Funding

This work was financially supported by the Water and Land Resource Center (WLRC), Addis Ababa University (AAU), Water Security and Sustainable Development Hub funded by the UK Research and Innovation's Global Challenges Research Fund (GCRF): ES/S008179/1.

Data Availability Statement

The original contributions presented in the study are included in the article; further inquiries can be directed to the corresponding author.

Acknowledgements

The authors extend their thanks to Water Security and Sustainable Development Hub the UK Research and Innovation's Global Challenges Research Fund (GCRF) for funding this research through the funding number ES/S008179/1.

Conflicts of Interest

The authors declare no conflict of interest.

References

- [1] Morris, B.G.L., Fan, J., 1997. Reservoir sedimentation handbook—design and management of dams, reservoirs, and watershed for sustainable use. McGraw-Hill: New York, NY, USA. pp. 481–482.
- [2] Adhami, M., Sadeghi, S.H., 2016. Sub-watershed prioritization based on sediment yield using game the-

- ory. *Journal of Hydrology*. 541(Part B), 977–987. DOI: <https://doi.org/10.1016/j.jhydrol.2016.08.008>
- [3] Assegide, E., Shiferaw, H., Tibebe, D., et al., 2023. Spatiotemporal dynamics of water quality indicators in Koka Reservoir, Ethiopia. *Remote Sensing*. 15(4), 1155. DOI: <https://doi.org/10.3390/rs15041155>
- [4] Abhachire, L.W., 2014. Studies on hydrobiological features of Koka Reservoir and Awash River in Ethiopia. *International Journal of Fisheries and Aquatic Studies*. 1(3), 158–162. Available from: <http://www.fisheriesjournal.com>
- [5] Girma, K., 2016. The state of freshwaters in Ethiopia. In *Freshwater*. Mount Holyoke College: South Hadley, MA, USA, pp. 137–188.
- [6] Argaw, M., Yohannes, H., 2024. Impact of land use/land cover changes on surface water and soil-sediment export in the urbanized Akaki River catchment, Awash Basin, Ethiopia. *Journal of Hydrology: Regional Studies*. 52, 101677. DOI: <https://doi.org/10.1016/j.ejrh.2024.101677>
- [7] Getaneh, Y., Abera, W., Abegaz, A., et al., 2022. A systematic review of studies on freshwater lakes of Ethiopia. *Journal of Hydrology: Regional Studies*. 44, 101250. DOI: <https://doi.org/10.1016/j.ejrh.2022.101250>
- [8] Assegide, T., Alamirew, Y.T., Dile, H., et al., 2022. A Synthesis of Surface Water Quality in Awash Basin, Ethiopia. *Frontiers in Water*. 4, pp. 1–17. DOI: <https://doi.org/10.3389/frwa.2022.782124>
- [9] Desta, L.T., 2005. Reservoir siltation in Ethiopia: Causes, source areas, and management options. Cuvillier Verlag: Göttingen, Germany. pp. 1960–2010. Available from: https://www.zefc.de/fileadmin/webfiles/downloads/zefc_ecology_development/ecol_dev_30_text.pdf
- [10] Hurni, H., 1993. Land degradation, famine, and land resource scenarios in Ethiopia. In: Pimentel, D. (ed.). *World Soil Erosion and Conservation*. Cambridge University Press: Cambridge, UK. pp. 27–61. Available from: https://www.researchgate.net/publication/279605109_Land_degradation_famine_and_land_resource_scenarios_in_Ethiopia#fullTextFileContent
- [11] Verstraeten, G., Poesen, J., de Vente, J., et al., 2003. Sediment yield variability in Spain: A quantitative and semiquantitative analysis using reservoir sedimentation rates. *Geomorphology*. 50(4), 327–348, DOI: [https://doi.org/10.1016/S0169-555X\(02\)00220-9](https://doi.org/10.1016/S0169-555X(02)00220-9)
- [12] Tullu, K.T., 2024. Assessment of soil erosion response to climate change in the Sululta catchment, Abbay Basin, Ethiopia. *H2 Open Journal*. 7(1), 1–37. DOI: <https://doi.org/10.2166/h2oj.2023.083>
- [13] Zhang, X., He, J., Deng, Z., et al., 2018. Comparative changes of influence factors of rural residential area based on spatial econometric regression model: A case study of Lishan Township, Hubei Province, China. *Sustainability*. 10(10), 3403. DOI: <https://doi.org/10.3390/su10103403>
- [14] Gantulga, N., Iimaa, T., Batmunkh, M., et al., 2023. Impacts of natural and anthropogenic factors on soil erosion. *Proceedings of the Mongolian Academy of Sciences*. 63(02), 3–18. DOI: <https://doi.org/10.5564/pmas.v63i02.1416>
- [15] Wang, A., Zhang, M., Ren, B., et al., 2023. Ventilation analysis of urban functional zoning based on circuit model in Guangzhou in winter, China. *Urban Climate*. 47, 1–9. DOI: <https://doi.org/10.1016/j.uclim.2022.101385>
- [16] De Boer, D.H., Crosby, G., 1996. Specific sediment yield and drainage basin scale. *IAHS-AISH Publication*. 236, 333–338.
- [17] Schiefer, E., Slaymaker, O., Klinkenberg, B., 2001. Physiographically controlled allometry of specific sediment yield in the Canadian Cordillera: A lake sediment-based approach. *Geografiska Annaler*. 83(1–2), 55–65. DOI: <https://doi.org/10.1111/j.0435-3676.2001.00144.x>
- [18] Houser, C., Hamilton, S., 2009. Sensitivity of post-hurricane beach and dune recovery to event frequency. *Earth Surface Processes and Landforms*. 34(5), 613–628. DOI: <https://doi.org/10.1002/esp.1730>
- [19] Rymbai, P.N., 2012. Estimation of sediment production rate of the Umbanun Micro-watershed, Meghalaya, India. *Journal of Geography and Regional Planning*. 5(11), 293–297. DOI: <https://doi.org/10.5897/jgrp11.032>
- [20] Tuppad, S., Shetty, G.R., Souravi, K., et al., 2017. Character association for fruit yield and yield traits in holostemma ada-kodien schult—A vulnerable medicinal plant. *Indian Journal of Ecology*. 44(2), 337–339.
- [21] Biswas, S., Sudhakar, S., Desai, V.R., 1999. Prioritisation of subwatersheds based on morphometric analysis of drainage basin: A remote sensing and GIS approach. *Journal of the Indian Society of Remote Sensing*. 27(3), 155–166. DOI: <https://doi.org/10.1007/BF02991569>
- [22] Degfe, A., Tilahun, A., Bekele, Y., et al., 2023. Adoption of soil and water conservation technologies and its effects on soil properties: Evidences from Southwest Ethiopia. *Heliyon*. 9(7), e18332. DOI: <https://doi.org/10.1016/j.heliyon.2023.e18332>
- [23] Shawul, A.A., Chakma, S., 2019. Spatiotemporal detection of land use/land cover change in the large basin using integrated approaches of remote sensing and GIS in the Upper Awash basin, Ethiopia. *Environmental Earth Sciences*. 78(5), 1–13. DOI: <https://doi.org/10.1007/s12665-019-8154-y>
- [24] Bekele, T., 2019. Effect of land use and land cover changes on soil erosion in Ethiopia. *International Journal of Agricultural Science and Food Technology*. 5, 26–34. DOI: <https://doi.org/10.17352/2455-815x.000038>

- [25] Dewan, A.M., Yamaguchi, Y., 2009. Using remote sensing and GIS to detect and monitor land use and land cover change in Dhaka Metropolitan of Bangladesh during 1960–2005. *Environmental Monitoring and Assessment*. 150(1–4), 237–249. DOI: <https://doi.org/10.1007/s10661-008-0226-5>
- [26] Wilson, E.H., Hurd, J.D., Civco, D.L., et al., 2003. Development of a geospatial model to quantify, describe and map urban growth. *Remote Sensing of Environment*. 86(3), 275–285. DOI: [https://doi.org/10.1016/S0034-4257\(03\)00074-9](https://doi.org/10.1016/S0034-4257(03)00074-9)
- [27] Miku, A.B., Meresa, G.A., Mulu, T., et al., 2023. Examining the impacts of climate variabilities and land use change on hydrological responses of Awash River basin, Ethiopia. *HydroResearch*. 6, 16–28. DOI: <https://doi.org/10.1016/j.hydres.2022.12.002>
- [28] Moges, A.S., Wondimagegn, S.A., Getahun, Y.S., 2024. Evaluate the effectiveness of soil and water conservation interventions in the upper Awash Basin, Ethiopia. *World Water Policy*. 10(1), 324–340. DOI: <https://doi.org/10.1002/wwp2.12165>
- [29] Vaidyanathan, R.K., Ramaraj, M., 2021. Prioritization of sub-watersheds in the Arasalar-Palavar region using Sediment Production Rate (SPR). *Indian Journal of Ecology*. 48(4), 1005–1010.
- [30] Ranjan, R., Jhariya, G., Jaiswal, R.K., 2013. Saaty's analytical hierarchical process based prioritization of sub-watersheds of Bina river basin using remote sensing and GIS. *American Scientific Research Journal for Engineering, Technology, and Sciences (ASRJETS)*. 3, 36–55.
- [31] Pandey, A., Chowdary, V.M., Mal, B.C., 2007. Identification of critical erosion prone areas in the small agricultural watershed using USLE, GIS and remote sensing. *Water Resour Manage*. 21(4), 729–746. DOI: <https://doi.org/10.1007/s11269-006-9061-z>
- [32] Beven, K., Wood, E., Sivapalan, M., 1998. Catchment morphology and hydrological processes are inextricably linked through the geomorphic processes of soil development, erosion and deposition. Water provides the major driving force in the development of morphology through its role as a transport. *Journal of Hydrology*. 100, 353–375.
- [33] Duressa, A.A., Feyissa, T.A., Tukura, N.G., et al., 2024. Identification of soil erosion-prone areas for effective mitigation measures using a combined approach of morphometric analysis and geographical information system. *Results in Engineering*. 21, 101712. DOI: <https://doi.org/10.1016/j.rineng.2023.101712>
- [34] Okoli, J., Nahazanan, H., Nahas, F., et al., 2023. High-resolution LIDAR-derived DEM for landslide susceptibility assessment using AHP and fuzzy logic in Serdang, Malaysia. *Geosciences*. 13(2), 34. DOI: <https://doi.org/10.3390/geosciences13020034>
- [35] Saha, S., Gayen, A., Pourghasemi, H.R., et al., 2019. Identification of soil erosion-susceptible areas using fuzzy logic and analytical hierarchy process modeling in an agricultural watershed of Burdwan district, India. *Environmental Earth Sciences*. 78(23), 649. DOI: <https://doi.org/10.1007/s12665-019-8658-5>
- [36] Sahour, H., Gholami, V., Vazifedan, M., et al., 2021. Machine learning applications for water-induced soil erosion modeling and mapping. *Soil and Tillage Research*. 211, 105032. DOI: <https://doi.org/10.1016/j.still.2021.105032>
- [37] Abdeta, G.C., Tesemma, A.B., Tura, A.L., et al., 2020. Morphometric analysis for prioritizing sub-watersheds and management planning and practices in Gidabo Basin, Southern Rift Valley of Ethiopia. *Applied Water Science*. 10(7), 1–15. DOI: <https://doi.org/10.1007/s13201-020-01239-7>
- [38] Meshram, S.G., Sharma, S.K., 2017. Prioritization of watershed through morphometric parameters: a PCA-based approach. *Applied Water Science*. 7(3), 1505–1519. DOI: <https://doi.org/10.1007/s13201-015-0332-9>
- [39] Javed, A., Khanday, M.Y., Ahmed, R., 2009. Prioritization of sub-watersheds based on morphometric and land use analysis using Remote Sensing and GIS techniques. *Journal of the Indian Society of Remote Sensing*. 37(2), 261–274. DOI: <https://doi.org/10.1007/s12524-009-0016-8>
- [40] Suj, V.R., Sheeja, R.V., Karuppasamy, S., 2015. Prioritization using morphometric analysis and land use/land cover parameters for Vazhichal watershed using remote sensing and GIS techniques. *International Journal for Innovative Research in Science & Technology*. 2(1), 61–68. Available from: <http://ijirst.org/articles/IJIRSTV2I1013.pdf>
- [41] Shekar, P.R., Mathew, A., 2022. Morphometric analysis for prioritizing sub-watersheds of Murredu River basin, Telangana State, India, using a geographical information system. *Journal of Engineering and Applied Science*. 69(1), 1–30. DOI: <https://doi.org/10.1186/s44147-022-00094-4>
- [42] Dabral, P.P., Baithuri, N., Pandey, A., 2008. Soil erosion assessment in a hilly catchment of North Eastern India using USLE, GIS and remote sensing. *Water Resources Management*. 22(12), 1783–1798. DOI: <https://doi.org/10.1007/s11269-008-9253-9>
- [43] Opricovic, S., Tzeng, G.H., 2004. Compromise solution by MCDM methods: A comparative analysis of VIKOR and TOPSIS. *European Journal of Operational Research*. 156(2), 445–455. DOI: [https://doi.org/10.1016/S0377-2217\(03\)00020-1](https://doi.org/10.1016/S0377-2217(03)00020-1)
- [44] Huang, J.J., Tzeng, G.H., Liu, H.H., 2009. A revised vikor model for multiple criteria decision making - The perspective of regret theory. *Communications in Computer and Information Science*. 35, 761–768. DOI: https://doi.org/10.1007/978-3-642-02298-2_112

- [45] Ameri, A., Pourghasemi, H., Cerda, A., 2018. Erodibility prioritization of sub-watersheds using morphometric parameters analysis and its mapping: A comparison among TOPSIS, VIKOR, SAW, and CF multicriteria decision making models. *Science of the Total Environment*. 613–614, 1385–1400. DOI: <https://doi.org/10.1016/j.scitotenv.2017.09.210>
- [46] Kang, D., Park, Y., 2014. Review-based measurement of customer satisfaction in mobile service: Sentiment analysis and VIKOR approach. *Expert Systems with Applications*. 41(4), 1041–1050. DOI: <https://doi.org/10.1016/j.eswa.2013.07.101>
- [47] Mir, A.A., Ahmed, R., 2021. SWAT based prioritization of sub-watersheds in Pohru watershed of Jhelum basin, northwestern Himalayas. *Research Journal of Agricultural Sciences*. 12, 1308–1315. DOI: <https://doi.org/10.5281/zenodo.5153487>
- [48] Tripathi, M.P., Panda, R.K., Raghuwanshi, N.S., 2003. Identification and prioritisation of critical sub-watersheds for soil conservation management using the SWAT model. *Biosystems Engineering*. 85(3), 365–379. DOI: [https://doi.org/10.1016/S1537-5110\(03\)00066-7](https://doi.org/10.1016/S1537-5110(03)00066-7)
- [49] Mishra, A., Kar, S., Singh, V.P., 2007. Prioritizing structural management by quantifying the effect of land use and land cover on watershed runoff and sediment yield. *Water Resources Management*. 21(11), 1899–1913. DOI: <https://doi.org/10.1007/s11269-006-9136-x>
- [50] Admas, B.F., Gashaw, T., Adem, A.A., et al., 2022. Identification of soil erosion hot-spot areas for prioritization of conservation measures using the SWAT model in Ribb watershed, Ethiopia. *Resources, Environment and Sustainability*. 8, 100059. DOI: <https://doi.org/10.1016/j.resenv.2022.100059>
- [51] Dibaba, W.T., Demissie, T.A., Miegel, K., 2021. Prioritization of sub-watersheds to sediment yield and evaluation of best management practices in highland ethiopia, finchaa catchment. *Land*. 10(6), 650. DOI: <https://doi.org/10.3390/land10060650>
- [52] Issaka, S., Ashraf, M.A., 2017. Impact of soil erosion and degradation on water quality: A review. *Geology, Ecology, and Landscapes*. 1(1), 1–11. DOI: <https://doi.org/10.1080/24749508.2017.1301053>
- [53] Takele, L., Kebede, M., 2018. Streamflow modeling of Upper Awash River Basin using soil and water assessment tool. *Applied Journal of Environmental Engineering Science*. 4, 456–466.
- [54] Mekonnen, T.M., Mitiku, A.B., Woldemichael, A.T., 2023. Flood hazard zoning of Upper Awash River Basin, Ethiopia, using the analytical hierarchy process (AHP) as compared to sensitivity analysis. *The Scientific World Journal*. 2023(2), 1-15. DOI: <https://doi.org/10.1155/2023/1675634>
- [55] High, C.E., Vecchi, V.V., Valdarno, S.G., 2016. Assessment of gully erosion in the Upper Awash, Central Ethiopian highlands based on a comparison of archived aerial photographs and very high resolution satellite images. *Physical Geography and Quaternary Dynamics*. 39, 161–170.
- [56] Salvini, R., Riccucci, S., Francioni, M., 2012. Topographic and geological mapping in the prehistoric area of Melka Kunture (Ethiopia). *Journal of Maps*. 8(2), 169–175. DOI: <https://doi.org/10.1080/17445647.2012.680779>
- [57] Gallotti, R., 2013. An older origin for the Acheulean at Melka Kunture (Upper Awash, Ethiopia): Techno-economic behaviours at Garba IVD. *Journal of Human Evolution*. 65(5), 594–620. DOI: <https://doi.org/10.1016/j.jhevol.2013.07.001>
- [58] Raynal, J., Kieffer, G., 2004. Lithology, dynamism and volcanic successions at Melka Kunture (Upper Awash, Ethiopia). In: Chavaillon, J., Piperno, M. (Eds.). *Studies on the Early Paleolithic site of Melka Kunture, Ethiopia*. Istituto Italiano di Preistoria e Protostoria: Rome, Italy. pp. 111–135. Available from: <http://halshs.archives-ouvertes.fr/halshs-00003990/>
- [59] Tolera, M.B., Chung, I.M., Chang, S.W., 2018. Evaluation of the climate forecast system reanalysis weather data for watershed modeling in Upper Awash Basin, Ethiopia. *Water (Switzerland)*. 10(6), 725. DOI: <https://doi.org/10.3390/w10060725>
- [60] Moriasi, D.N., Arnold, J.G., Van Liew, M.W., et al., 2007. Model evaluation guidelines for systematic quantification of accuracy in watershed simulations. *Transactions of the ASABE*. 50(3), 885–900. DOI: <https://doi.org/10.13031/2013.23153>
- [61] Veltman, K., Alan, R.C., Larry, C., et al., 2018. A quantitative assessment of Beneficial Management Practices to reduce carbon and reactive nitrogen footprints and phosphorus losses on dairy farms in the US Great Lakes region. *Agricultural Systems*. 166, 10–25. DOI: <https://doi.org/10.1016/j.agsy.2018.07.005>
- [62] Ali, S.A., Ikbali, J., 2015. Prioritization based on geomorphic characteristics of Ahar watershed, Udaipur district, Rajasthan, India using Remote Sensing and GIS. *Journal of Environmental Research And Development*. 10(1), 187–200. Available from: https://www.researchgate.net/publication/281856622_Prioritization_based_on_geomorphic_characteristics_of_Ahar_watershed_Udaipur_districtRajasthan_India_using_Remote_Sensing_and_GIS
- [63] Jha, M., Gassman, P.W., Secchi, S., et al., 2004. Effect of watershed subdivision on swat flow, sediment, and nutrient predictions. *Journal of the American Water Resources Association*. 40(3), 811–825. DOI: <https://doi.org/10.1111/j.1752-1688.2004.tb04460.x>
- [64] Arabi, M., Govindaraju, R.S., Hantush, M.M., et al., 2006. Role of watershed subdivision on modeling the effectiveness of best management practices With SWAT. *Water Resources*. 42(2), 513–528.

- [65] Lin, B., Chen, X., Yao, H., 2020. Threshold of sub-watersheds for SWAT to simulate hillslope sediment generation and its spatial variations. *Ecological Indicators*. 111(8), 106040. DOI: <https://doi.org/10.1016/j.ecolind.2019.106040>
- [66] Farhan, Y., Anbar, A., Enaba, O., et al., 2015. Quantitative analysis of geomorphometric parameters of Wadi Kerak, Jordan, using remote sensing and GIS. *Journal of Water Resource and Protection*. 7(6), 456–475. DOI: <https://doi.org/10.4236/jwarp.2015.76037>
- [67] Rahman, S.A., Ajeez, S.A., Aruchamy, S., et al., 2015. Prioritization of sub watershed based on morphometric characteristics using Fuzzy Analytical Hierarchy Process and Geographical Information System—A study of kallar watershed, Tamil Nadu. *Aquatic Procedia*. 4, 1322–1330. DOI: <https://doi.org/10.1016/j.aqpro.2015.02.172>
- [68] Strahler, A.N., 1973. *Geological society of America Bulletin*. Geological Society Of America Bulletin. 11, 1117–1142. DOI: [https://doi.org/10.1130/0016-7606\(1952\)63](https://doi.org/10.1130/0016-7606(1952)63)
- [69] Horton, R.E., 1945. Erosional development of streams and their drainage basins, hydrophysical approach to quantitative morphology. *Geological Society of America Bulletin*. 37(12), 555–558. DOI: [https://doi.org/10.1130/0016-7606\(1945\)56](https://doi.org/10.1130/0016-7606(1945)56)
- [70] Schumm, S.A., 1956. Evolution of drainage systems and slopes in badlands at Perth Amboy, New Jersey. *Geological society of America bulletin*. 67(5), 597–646.
- [71] Patton, P.C., Baker, V.R., 1976. Morphometry and floods in small drainage basins subject to diverse hydrogeomorphic controls. *Water Resources Research*. 12(5), 941–952. DOI: <https://doi.org/10.1029/WR012i005p00941>
- [72] Strahler, A.N., 1957. Quantitative analysis of watershed geomorphology, transactions of the American Geophysical Union. *Transactions, American Geophysical Union*. 38(6), 913–920.
- [73] Horton, R.E., 1932. Drainage-basin characteristics. *Transactions American Geophysical Union*. 13(1), 350–361. DOI: <https://doi.org/10.1029/TR013i001p00350>
- [74] Smith, K.G., 1950. Standards for grading texture of erosional topography. *American Journal of Science*. 248, 655–668. DOI: <https://sci-hub.ru/https://doi.org/10.2475/ajs.248.9.655>
- [75] Schumm, S.A., 1963. Geological Society of America Bulletin sequences in the cratonic interior of North America. *Geological Society of America Bulletin*. 74(2), 93–114. DOI: [https://doi.org/10.1130/0016-7606\(1963\)74](https://doi.org/10.1130/0016-7606(1963)74)
- [76] Rai, P., Mishra, V.N., Mohan, K., 2017. A study of morphometric evaluation of the Son basin, India using geospatial approach. *Remote Sensing Applications: Society and Environment*. 7, 9–20. DOI: <https://doi.org/10.1016/j.rsase.2017.05.001>
- [77] Adu, J.T., Kumarasamy, M.V., 2018. Assessing non-point source pollution models: A review. *Polish Journal of Environmental Studies*. 27(5), 1913–1922. DOI: <https://doi.org/10.15244/pjoes/76497>
- [78] Santhi, C., Arnold, J.G., Williams, J.R., et al., 2001. Application of a watershed model to evaluate management effects on point and nonpoint source pollution. *Transactions of the ASAE. American Society of Agricultural Engineers*. 44(76502), 1559–1570.
- [79] Ganasri, B.P., 2015. A review on hydrological models. *Aquatic Procedia*. 4, 1001–1007. DOI: <https://doi.org/10.1016/j.aqpro.2015.02.126>
- [80] Yang, Y.S., Wang, L., 2010. A review of modelling tools for implementation of the EU water framework directive in handling diffuse water pollution. *Water Resources Management*. 24(9), 1819–1843. DOI: <https://doi.org/10.1007/s11269-009-9526-y>
- [81] Renard, K., Foster, G.R., Weesies, G., et al., 1997. Predicting soil erosion by water: A guide to conservation planning with the Revised Universal Soil Loss Equation (RUSLE). *Agriculture Handbook Number 703*. Available from: <https://www3.epa.gov/npdes/pubs/ruslech2.pdf> (cited 24 January 2023).
- [82] Arnold, J.G., Moriasi, D., Gassman, P., et al., 2012. SWAT: Model use, calibration, and validation. *Transactions of the ASABE*. 55(4), 1249–1260. DOI: <https://doi.org/10.13031/2013.42256>
- [83] Winchell, M.F., Peranginangin, N., Srinivasan, R., et al., 2018. Soil and Water Assessment Tool model predictions of annual maximum pesticide concentrations in high vulnerability watersheds. *Integrated Environmental Assessment and Management*. 14(3), 358–368. DOI: <https://doi.org/10.1002/ieam.2014>
- [84] Gholami, A., Habibnejad Roshan, M., Shahedi, K., et al., 2016. Hydrological stream flow modeling in the Talar catchment (central section of the Alborz Mountains, north of Iran): Parameterization and uncertainty analysis using SWAT-CUP. *Journal of Water and Land Development*. 30(1), 57–69. DOI: <https://doi.org/10.1515/jwld-2016-0022>
- [85] Abbaspour, K.C., 2012. A package of calibration procedures linked to SWAT through a generic platform to perform calibration, validation, and uncertainty analysis SWAT-CUP. *enviroGRIDS – FP7 European project*. pp. 1–104. Available from: https://envirogrids.net/envirogrids_d4.5_calibration_swat_cupdfb0.pdf?option=com_jdownloads&Itemid=13&view=finish&cid=145&catid=13
- [86] Abbaspour, K.C., Yang, J., Maximov, I., et al., 2007. Modelling hydrology and water quality in the pre-alpine/alpine Thur watershed using SWAT. *Journal of Hydrology*. 333(2–4), 413–430. DOI: <https://doi.org/10.1016/j.jhydrol.2006.09.014>
- [87] Im, S., Brannan, K.M., Mostaghimi, S., et al., 2007.

- Comparison of HSPF and SWAT models performance for runoff and sediment yield prediction. *Journal of Environmental Science and Health*. 42(11), 1561–1570. DOI: <https://doi.org/10.1080/10934520701513456>
- [88] Sasanka, C.T., Ravindra, K., 2015. Implementation of VIKOR method for selection of magnesium alloy to suit automotive applications. *International Journal of Advanced Science and Technology*. 83, 49–58. DOI: <https://doi.org/10.14257/ijast.2015.83.05>
- [89] Wang, C., Pang, C., 2011. Using VIKOR method for evaluating service quality of online auction under fuzzy environment. *IJCSET*. 1(6), 307–314.
- [90] Xue, M., Tang, X., Feng, N., 2016. An extended VIKOR method for multiple attribute decision analysis with bidimensional dual hesitant fuzzy information. *Mathematical Problems in Engineering*. 2016(1), 16. DOI: <https://doi.org/10.1155/2016/4274690>
- [91] Pant, S., Kumar, A., Ram, M., et al., 2022. Consistency indices in analytic hierarchy process: A review. *Mathematics*. 10(8), 1–15. DOI: <https://doi.org/10.3390/math10081206>
- [92] Saaty, T.L., 1977. A scaling method for priorities in hierarchical structures. *Journal of mathematical psychology*. 15(3), 234–281. DOI: [https://doi.org/10.1016/0022-2496\(77\)90033-5](https://doi.org/10.1016/0022-2496(77)90033-5)
- [93] Suh, Y., Park, Y., Kang, D., 2019. Evaluating mobile services using integrated weighting approach and fuzzy VIKOR. *PLoS One*. 14(6), 1–28. DOI: <https://doi.org/10.1371/journal.pone.0217786>
- [94] Topno, A.R., Job, M., Rusia, D.K., et al., 2022. Prioritization and identification of vulnerable sub-watersheds using morphometric analysis and an integrated AHP-VIKOR method. *Water Supply*. 22(11), 8050–8064. DOI: <https://doi.org/10.2166/ws.2022.303>
- [95] Ren, J., Manzardo, A., Mazzi, A., et al., 2015. Prioritization of bioethanol production pathways in China based on life cycle sustainability assessment and multi-criteria decision-making. *International Journal of Life Cycle Assessment*. 20(6), 842–853. DOI: <https://doi.org/10.1007/s11367-015-0877-8>
- [96] Saaty, R.W., 1987. The analytic hierarchy process—what it is and how it is used. *Mathematical Modelling*. 9(3–5), 161–176. DOI: [https://doi.org/10.1016/0270-0255\(87\)90473-8](https://doi.org/10.1016/0270-0255(87)90473-8)
- [97] Saaty, T.L., Vargas, L.G., 1987. Stimulus-response with reciprocal kernels: The rise and fall of sensation. *Journal of Mathematical Psychology*. 31(1), 83–92. DOI: [https://doi.org/10.1016/0022-2496\(87\)90037-X](https://doi.org/10.1016/0022-2496(87)90037-X)
- [98] Saaty, T.L., 1990. How to make a decision: The analytic hierarchy process. *European Journal of Operational Research*. 48(1), 9–26. DOI: [https://doi.org/10.1016/0377-2217\(90\)90057-I](https://doi.org/10.1016/0377-2217(90)90057-I)
- [99] Ratnam, K.N., Srivastava, Y.K., Venkateswara Rao, V., et al., 2005. Check dam positioning by prioritization micro-watersheds using SYI model and morphometric analysis—remote sensing and GIS perspective. *Journal of the Indian Society of Remote Sensing*. 33(1), 25–38. DOI: <https://doi.org/10.1007/BF02989988>
- [100] Krisper, M., 2021. Problems with Risk Matrices Using Ordinal Scales. Available from: <http://arxiv.org/abs/2103.05440>
- [101] Metcalf, J., Peterson, L., Carrasquillo, R., et al., 2012. National Aeronautics and Space Administration (NASA) Environmental Control and Life Support (ECLS) Integrated Roadmap Development. In *Proceedings of the 42nd International Conference on Environmental Systems*; San Diego, CA, USA; 15–19 July 2012. p. 3444.
- [102] Nitheshnirmal, S., Bhardwaj, A., Dineshkumar, C., et al., 2019. Prioritization of erosion prone micro-watersheds using morphometric analysis coupled with multi-criteria decision making. *Proceedings*. 24(1), 11. DOI: <https://doi.org/10.3390/iecg2019-06207>
- [103] Gumma, M.K., Birhanu, B.Z., Mohammed, I.A., et al., 2016. Prioritization of watersheds across mali using remote sensing data and GIS techniques for agricultural development planning. *Water (Switzerland)*. 8(6), 1–17. DOI: <https://doi.org/10.3390/W8060260>
- [104] Dofee, A.A., Chand, P., Kumar, R., 2024. Prioritization of soil erosion-prone sub-watersheds using geomorphometric and statistical-based weighted sum priority approach in the middle Omo-Gibe River basin, Southern Ethiopia. *International Journal of Digital Earth*. 17(1), 1–32. DOI: <https://doi.org/10.1080/17538947.2024.2350198>
- [105] Makhdumi, W., Dwarakish, G.S., 2019. Prioritisation of watersheds using TOPSIS and VIKOR method. In *Proceedings of the SPIE 11174, Seventh International Conference on Remote Sensing and Geoinformation of the Environment (RSCy2019)*; Paphos, Cyprus; 27 June 2019. p. 6. DOI: <https://doi.org/10.1117/12.2532024>
- [106] Nasir, M.J., Ahmad, W., Jun, C., et al., 2023. Soil erosion susceptibility assessment of Swat River sub-watersheds using the morphometry-based compound factor approach and GIS. *Environmental Earth Sciences*. 82(12), 1–28. DOI: <https://doi.org/10.1007/s12665-023-10982-4>
- [107] Gela, A.G., Mengistu, D.A., Maru, S., et al., 2020. Watershed Prioritization Using Morphometric Analysis & RUSLE Model for Soil Conservation Planning, in *Gilgel Abay Watershed, Ethiopia*, 15 December 2020, PREPRINT (Version 1) available at Research Square. DOI: <https://doi.org/10.21203/rs.3.rs-126047/v1>
- [108] Biswas, S.S., 2016. Analysis of GIS based morphometric parameters and hydrological changes in Parbati River basin, Himachal Pradesh, India. *Journal of Geography & Natural Disasters*. 6(2), 1–8. DOI: <https://doi.org/10.4172/2167-0587.1000175>

- [109] Sethupathi, A.S., Lakshmi, N., Vasanthamohan, V., et al., 2011. Prioritization of mini watersheds based on morphometric analysis using remote sensing and GIS in a drought prone Bargur Mathur sub watersheds, Ponnaiyar River basin, India. *International Journal of Geomatics and Geosciences*. 2(2), 403–414.
- [110] Singh, A.P., Arya, A.K., Sen Singh, D., 2020. Morphometric analysis of Ghaghara River basin, India, using SRTM data and GIS. *Journal of the Geological Society of India*. 95(2), 169–178. DOI: <https://doi.org/10.1007/s12594-020-1406-3>
- [111] Hindersah, R., Handyman, Z., Indriani, F.N., et al., 2018. Azotobacter population, soil nitrogen and groundnut growth in mercury-contaminated tailing inoculated with Azotobacter. *Journal of Degraded Andmining Landsmanagement*. 5(53), 2502–2458. DOI: <https://doi.org/10.15243/jdmlm>
- [112] Paghadal, A.M., Rank, H.D., Makavana, J.M., et al., 2019. Quantitative analysis of geomorphometric parameters of Ozat River basin using remote sensing and GIS. *International Journal of Current Microbiology and Applied Sciences*. 8(09), 213–233. DOI: <https://doi.org/10.20546/ijcmas.2019.809.027>
- [113] Langbein, W.B., 1947. Topographic characteristics of drainage basins. No. 968-C, USGPO. Available from: <http://pubs.usgs.gov/wsp/0968c/report.pdf> (cited 12 February 2022).
- [114] Sukristiyanti, S., Maria, R., Lestiana, H., 2018. Watershed-based morphometric analysis: A review. *IOP Conference Series: Earth and Environmental Science*. 118(1), 1–6. DOI: <https://doi.org/10.1088/1755-1315/118/1/012028>
- [115] Rai, P.K., Chandel, R.S., Mishra, V.N., et al., 2018. Hydrological inferences through morphometric analysis of lower Kosi river basin of India for water resource management based on remote sensing data. *Applied Water Science*. 8(1), 1–16. DOI: <https://doi.org/10.1007/s13201-018-0660-7>
- [116] Sakthivel, R., Jawahar Raj, N., Sivasankar, V., et al., 2019. Geo-spatial technique-based approach on drainage morphometric analysis at Kalrayan Hills, Tamil Nadu, India. *Applied Water Science*. 9(1), 1–18. DOI: <https://doi.org/10.1007/s13201-019-0899-7>
- [117] Umrikar, B.N., 2017. Morphometric analysis of Andhale watershed, Taluka Mulshi, District Pune, India. *Applied Water Science*. 7(5), 2231–2243. DOI: <https://doi.org/10.1007/s13201-016-0390-7>
- [118] Patel, D.P., Gajjar, C.A., Srivastava, P.K., 2013. Prioritization of Malesari mini-watersheds through morphometric analysis: A remote sensing and GIS perspective. *Environmental Earth Sciences*. 69(8), 2643–2656. DOI: <https://doi.org/10.1007/s12665-012-2086-0>
- [119] Chopra, R., Dhiman, R.D., Sharma, P.K., 2005. Morphometric analysis of sub-watersheds in Gurdaspur district, Punjab using remote sensing and GIS techniques. *Journal of the Indian Society of Remote Sensing*. 33(4), 531–539. DOI: <https://doi.org/10.1007/BF02990738>
- [120] Nautiyal, M.D., 1994. Morphometric analysis of a drainage basin using aerial photographs: A case study of Khairkuli basin, district Dehradun, U.P. *Journal of the Indian Society of Remote Sensing*. 22(4), 251–261. DOI: <https://doi.org/10.1007/BF03026526>
- [121] Ahmed, S.A., Chandrashekarappa, K.N., Raj, S.K., et al., 2010. Evaluation of morphometric parameters derived from ASTER and SRTM DEM—A study on Bandihole sub-watershed basin in Karnataka. *Journal of the Indian Society of Remote Sensing*. 38(2), 227–238. DOI: <https://doi.org/10.1007/s12524-010-0029-3>
- [122] Vittala, S.S., Govindaiah, S., Gowda, H.H., 2004. Morphometric analysis of sub-watersheds in the Pavagada area of Tumkur district, South India using remote sensing and GIS techniques. *Journal of the Indian Society of Remote Sensing*. 32(4), 351–361.
- [123] Rai, P., Chaubey, P.K., Mohan, K., et al., 2017. Geoinformatics for assessing the inferences of quantitative drainage morphometry of the Narmada Basin in India. *Applied Geomatics*. 9(3), 167–189. DOI: <https://doi.org/10.1007/s12518-017-0191-1>
- [124] Das, A.K., Mukherjee, S., 2005. Drainage morphometry using satellite data and GIS in Raigad district, Maharashtra. *Journal of the Geological Society of India*. 65(5), 577–586.
- [125] Puno, G.R., Puno, R.C.C., 2019. Watershed conservation prioritization using geomorphometric and land use-land cover parameters. *Global Journal of Environmental Science and Management*. 5(3), 279–294. DOI: <https://doi.org/10.22034/gjesm.2019.03.02>
- [126] Abbaspour, K.C., Rouholahnejad, E., Vaghefi, S., et al., 2015. A continental-scale hydrology and water quality model for Europe: Calibration and uncertainty of a high-resolution large-scale SWAT model. *Journal of Hydrology*. 524, 733–752. DOI: <https://doi.org/10.1016/j.jhydrol.2015.03.027>
- [127] Moriasi, D.N., Gitau, M.W., Pai, N., et al., 2015. Hydrologic and water quality models: Performance measures and evaluation criteria. *Transactions of the ASABE*. 58(6), 1763–1785. DOI: <https://doi.org/10.13031/trans.58.10715>
- [128] Liu, X., Li, H., Zhang, S., et al., 2019. Gully erosion control practices in Northeast China: A review. *Sustainability*. 11(18), 1–16. DOI: <https://doi.org/10.3390/su11185065>
- [129] Welde, K., 2016. Identification and prioritization of subwatersheds for land and water management in Tekeze dam watershed, Northern Ethiopia. *International Soil and Water Conservation Research*. 4(1), 30–38. DOI: <https://doi.org/10.1016/j.iswcr.2016.02.006>
- [130] Kefay, T., Abdisa, T., Tumsa, B.C., 2022. Prioritiza-

tion of susceptible watershed to sediment yield and evaluation of Best Management Practice: A case study of Awata River, Southern Ethiopia. *Applied and Environmental Soil Science*. 2022(1), 1–16. DOI: <https://doi.org/10.1155/2022/1460945>

[131] Jothimani, M., Lawrence, F., Dawit, Z., 2020. Mor-

phometric analysis and prioritization of sub-watersheds for soil erosion using Geomatics technologies in Megech River catchment, Lake Tana Basin, North Western Ethiopia. *Ethiopian Journal of Science and Sustainable Development e-ISSN*. 8(1), 52–64. DOI: <https://doi.org/10.20372/ejssdastu:v8.i1.2021.225>